Meniscus Movement in Respiratory Airways

by

Kathleen S. MacKenzie

B.S., Mechanical Engineering
Northeastern University, 1990

Submitted to the Department of
Mechanical Engineering in partial fulfillment of
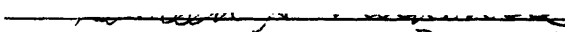the requirements for the
degree of

MASTER OF SCIENCE
in
Mechanical Engineering

at the

MASSACHUSETTS INSTITUTE OF TECHNOLOGY

June 1995

Signature of Author _____
Department of Mechanical Engineering
May 1995

Certified by _____
Professor Roger D. Kamm
Thesis Supervisor

Accepted by _____
Professor Ain A. Sonin
Chairman, Departmental Committee on Graduate Studies

MENISCUS MOVEMENT IN RESPIRATORY AIRWAYS

by

KATHLEEN S. MACKENZIE

ABSTRACT

An experimental investigation into liquid plug movement in small airways was completed to determine a relationship between the applied pressure gradient across the plug to the velocity of the plug, the rate the plug dissolves and the thickness of the film deposited on the airway wall. There are two physiological applications for this study - airway re-opening when closure is caused by a liquid plug and surfactant replacement therapy. The physical situtation was idealized by a single, long rigid tube in which a thin film of viscous fluid was deposited on the wall. A liquid plug was introduced and subjected to a pressure gradient. The velocity, dissipation rate and trailing film thickness were recorded. The results were non-dimensionalized and grouped by initial conditions (diameter, initial film thickness and initial plug length) and plotted against capillary number. The studies conclude that the deposited film thickness seems constant and therefore independent of capillary number. The faster moving plugs lose volume more rapidly and hence dissolve more quickly. The total pressure drop across the plug is relatively small compared to the pressure drop across a plug in a collapsed tube. The viscous pressure and capillary pressure contributions are significant to the total pressure drop across the plug.

Thesis Supervisor: Professor Roger Kamm

Title: Professor of Mechanical Engineering

At last I've graduated....

If it weren't for Professor Roger Kamm and his gentle yet persistent encouragement, I doubt it would have ever happened. I am indebted to him for his support and understanding from my acceptance through graduation. Thank you.

I'd also like to thank GE for the financial support and time off from work to complete my thesis and classes. I would especially like to thank Dave Reid, my immediate manager, for his understanding when I needed the extra time off at the end of the semester to complete my thesis.

Everyone in the Fluids Lab made the whole experience a lot of fun! Edwin, Naomi, Greg, Dave, Mariano, Arthur, Serhat, John, Frank and everyone else - the mountain biking, skiing and snow boarding, camping and the countless lunches were great - I'm sure we'll stay friends a long time.

Matt Monoghan and Paul Acquaviva... my friends and co-workers. Matt, the only person I know who finished the 'ABC' course and graduated from MIT on time, you are a great example of what hard work, discipline, and a never-wavering positive attitude can accomplish. I wish we could have graduated together, since we started together, but I needed the extra two years to.... to.... to really enjoy life as a student *and* full time employee. Paul provided that extra push in the end. When he said, "I'm going to see if I can graduate before you", I thought, "It's time I finish up." Sometimes it takes just one little thing to get you going again.

And last and most, I would like to thank my husband for his patience and encouragement through the whole process... from 'A' course through graduation. He was especially great caring for our 4 month old son during the last month of my final semester. He mastered the skills needed to make a GREAT dad and I love him very much for it.

Now it's time to move on and perhaps settle into family life... that'll be different...

List of Figures

List of Tables

4

Chapter 1

Introduction

There are two physiological applications motivating the study of meniscus behavior in small airways: airway re-opening and surfactant replacement therapy. Airway re-opening pertains to the removal of an occlusion which inhibits the free passage of air in a respiratory bronchiole. The occlusion may be due to a liquid plug or meniscus which develops from the film lining the airway walls or as Kamm and Schroter[1] suggest, the airway walls collapsing. Surfactant replacement therapy is performed on preterm infants born without sufficient lung surfactant. The therapy consists of injecting a slug of surfactant into the bronchial tree via the mouth, and allowing it to spread through out. Studying meniscus movement in respiratory airways will contribute to the understanding of how a slug of surfactant dissipitates and spreads through the lungs thereby helping to refine the replacement therapy, and contribute to the understanding of when a liquid plug might dissolve thus permitting the passage of air.

---

[1]Kamm, R.D., and Schroter, R.C., "Is airway closure caused by a liquid film instability?", *Resp. Physiol.* 75:141-156, 1989.

There are believed to be two mechanisms contributing to airway closure: 1) liquid bridge formation and 2) compliant collapse. Liquid bridging was first suggested by Macklem[2] in the early seventies and occurs when the fluid lining the airways forms a meniscus in the lumen obstructing the passage of air. Liquid bridging results from a surface tension induced instability in the thin liquid layer lining the airway walls. Kamm and Schroter experimentally quantified the conditions needed for closure, showing that a critical liquid-to-air volume ratio must be achieved before a bridge can form. A theoretical model predicting the time scale for closure was developed by Johnson et al.[3] and extended by Otis et al.[4] which simulates liquid bridging. Compliant collapse refers to the buckling of the airway wall, usually due to an increase in surface forces, a reduction in external tethering forces or a combination of the two. During expiration, the airway diameter decreases, thereby lowering the thin film pressure relative to the airway pressure. This increases the surface forces relative to the airway stiffness causing the airway to collapse. The film lining the airway then acts as a "viscous adhesive" holding the walls together. This occurs when the surface tension is large or the tube is very compliant. Investigations into both closure mechanisms (liquid bridging and compliant collapse) have increased the understanding of how closure might occur, and under what circumstances it may or may not occur. The next logical step in understanding airway occlusions is to consider when and under what circumstances re-opening may occur.

Gaver et al.[5] studied the re-opening of collapsed airways using a bench top model. They measured the relationship between the airway opening velocity and the applied pressure for different radii tubes using fluids of different surface tension and viscosity. Wall compliance

---

[2]Macklem, P.T, "Airway obstruction and collateral ventilation", *Physiol. Rev.*, 51: 368-385, 1971

[3]Johnson, M., Kamm, R.D., Ho, L.W., Shapiro, A., and Pedley, T.J., "The nonlinear growth of surface-tension-driven instabilities of a thin annular film", *J. Fluid Mech.*, 233:141-156, 1991.

[4]Otis, D.R, Johnson, M., Pedley, T.J., and Kamm, R.D., "The Role of Pulmonary Surfactant in Airway Closure: A Computational Study", J. Appl. Physiol, 1993

[5]Gaver, D.P., Samsel, R.W., Solway, J., "Effects of surface tension and viscosity on airway reopening", *J. Appl. Physiol.*, 69:74-85, 1990.

was mimicked by varying the axial tension on the tube, and the fluid film thickness was varied. Their experiments showed that when the capillary number (ratio of viscous to surface forces) is small (Ca < 0.5), the opening pressure is independent of viscous forces and is of order $8\sigma/R$ (where σ is the surface tension and R is the inflated tube radius). They also empirically derived a prediction for re-opening times. They predict that once the yield pressure ($8\sigma/R$) is exceeded, opening occurs instantly. However, for cases where the capillary number is large due to elevated film viscosity or surface tension, as is the case in diseased lungs, viscous forces increase the required pressure and time needed for re-opening, and no correlation or predictions are developed for these cases.

Gaver *et al.* focused on the re-opening of collapsed airways that closed into a "ribbon like region". They deposited a thin film of fluid on the tube walls and then pressurized a meniscus which traveled the length of the tube, forcing the walls apart. His work provides a great deal of insight into airway re-opening when the dominant closure mechanism is collapsed walls. But how applicable are his findings when liquid bridge formation is the dominant mechanism? Closure in the airway is a combination of the airway collapsing and a liquid plug developing. Therefore, to fully understand airway re-opening, one must also consider the behavior of the liquid bridge and the criteria for the meniscus to "break apart".

In this regard, Liu[6] *et al.* evaluated the resistance offered by a column of liquid being forced through a narrow section of tube. The column of liquid represents a liquid bridge or plug. Pressure was continuously increased to force the column of liquid into the narrow section of the tube. When the trailing meniscus reached the most constricted region, the driving pressure would rise to a peak, and then drop abruptly as the meniscus passed through the narrow section. The column would temporarily dissolve and the air was free to flow.

---

[6]Liu, M., Wang, L., Li, E., Enhorning, E., "Pulmonary surfactant will secure free airflow through a narrow tube", *J. Appl. Physiol.* 71(2): 742-748, 1991.

However, Liu found that the occlusion immediately reformed after the column was pushed through the narrow region. Liu was investigating under what circumstances the obstruction might or might not redevelop. He found that if the meniscus consisted of a small amount of calf surfactant the surface tension was sufficiently lowered to prohibit the bridge from reforming. He did not attempt to quantify the conditions needed to disperse the bridge or how rapidly the plug dissolved. He was simply considering surfactant's role in maintaining an open airway.

The present study quantifies the relationship between pressure, plug velocity, trailing film thickness and the rate the plug dissipates. Quantifying these parameters will define the criteria needed for plugs to dissipate. The dissipation is related to the change in the plug length and the film deposited on the tube wall. Film deposition has been studied extensively by many researchers. G.I. Taylor[7] quantified the fraction of a viscous fluid deposited on the tube walls when a finger of low viscosity fluid displaces it. He found the fraction asymptotically approaches .56 as the capillary number (ratio of viscous forces to surface forces) increased. His findings were supported by Cox[8] who refined the limiting value to be .6 for large capillary numbers (Ca > 10).

Other researchers looking into film deposition focused on conditions where the capillary numbers were small. Bretherton[9] studied the passage of a long inviscid bubble through a viscous fluid. He analytically derived the thickness of the film deposited on the tube wall and the pressure drop across the bubble using lubrication equations. The fraction of the viscous fluid deposited on the tube wall, 'W", he defined as:

[7]Taylor, G.I., "Deposition of a viscous fluid on the wall of a tube", *J. Fluid. Mech.*, 10:161, 1961.
[8]Cox, B.G., "On driving a viscous fluid out of a tube", *J. Fluid Mech*, 14:81-96, 1962.
[9]Bretherton, F.P., "The motion of long bubbles in tubes", *J. Fluid Mech.*, 10:166-188, 1961

$$W = 1.29\left(3\frac{\mu V}{\sigma}\right)^{2/3} \qquad \frac{\mu V}{\sigma} \to 0$$

and the pressure drop across the bubble he derived to be:

$$P = 3.58\left(3\frac{\mu V}{\sigma}\right)^{2/3} \qquad \frac{\mu V}{\sigma} \to 0$$

Bretherton experimentally verified the film thickness predictions, with discrepancies between theory and experimental becoming significant at very low bubble speeds (Ca < .003), in which case he under predicts the film thickness. The discrepancies between his theory and experiments, as explained by Ratulowski and Chang[10], are due to the Marangoni effect of small amounts of impurities in the film layer. Bretherton assumed the film layer is stationary, but Ratulowski and Chang showed that for slow bubbles, a mass concentration gradient exists in the film which sets up a surface traction drawing more fluid into the film. At higher bubble speeds, the horizontal velocity is large enough that the surface concentration gradient does not cause enough traction to alter the flow field. In the respiratory airways, it is assumed that the liquid slugs move with enough velocity that the marangoni affects can be neglected. Additional work to establish the deposited film thickness was completed by Schwartz et al.[11] who determined the average wetting film left by the passage of an air bubble to be a function of bubble length and speed. Schwartz again was looking at very low capillary numbers, Ca ~ 10^{-3}. For short bubbles, he found agreement with Bretherton's lubrication approximation, where the film thickness is

$$h_\infty = .643\,R\,(3\,Ca)^{2/3}$$

[10]Ratulowski, J., and Chang, H.-C., "Marangoni effects of trace impurities on the motion of long gas bubbles in capillaries", J. Fluid Mech., 210: 303-328, 1990

[11]Schwartz, L.W., Princen, H.M, and Kiss, A.D., "On the motion of bubbles in capillary tubes", J. Fluid Mech., 172: 259-275, 1986

For long bubbles, the film thickness was greater and independent of the bubble length.

Except for the work by Taylor and Cox, the research on film deposition has been limited to low capillary numbers, less than 10^{-3}. In respiratory bronchioles where a liquid bridge has developed or a slug of surfactant is introduced, it is difficult to predict what the capillary number might be, but one could expect it to be on order of 10^{-2}. The results of Bretherton and Taylor will be most applicable.

The primary objective of this study is to determine how a liquid plug behaves when subjected to a given pressure gradient. The introduction of a slug of surfactant or the condition of a closed airway due to a liquid bridge has been idealized by considering a single, long rigid tube. In these experiments a thin layer of viscous fluid pre-exists on the tube walls. A plug of the same viscous liquid is introduced and subjected to a pressure gradient. As the slug translates down the tube, its length decreases as additional film is deposited on the walls. These experiments correlate the velocity of the plug, the rate it changes length and the increase in film thickness to the applied pressure and initial conditions. This will provide useful information when studying how an airway obstructed by a liquid bridge re-opens and how a surfactant slug is deposited on the airway walls.

Chapter 2

Methods

Experimental.

Experiments were conducted to determine how far a liquid plug will travel before it dissolves and what pressures are required to make the meniscus move. As the meniscus translates down the tube, it deposits a thin film on the tube walls. The meniscus movement and its dissipation is characterized by the change in the plug length (dL/dt), the plug axial velocity (V_p) and the trailing film thickness deposited on the wall of the tube (h(t)). The important parameters are the tube diameter (D), the initial film thickness (h_o), the initial slug length (L_o), the pressure gradient (Δp), and the fluid properties surface tension (σ) and viscosity (μ).
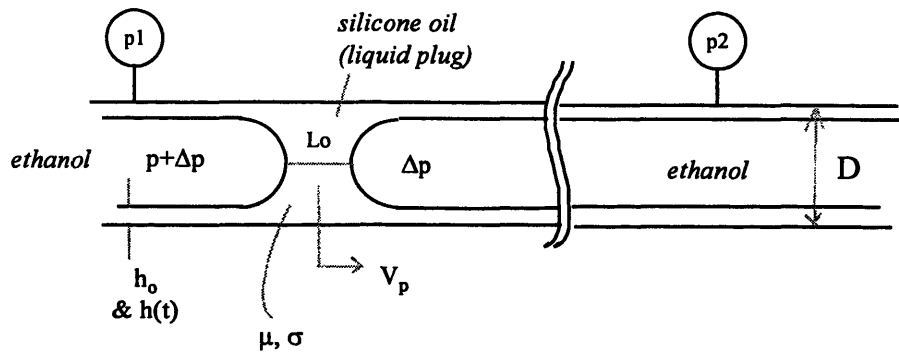
Figure 1. Important dimensional parameters

11

Apparatus. A straight plexiglas tube with a 1.24 cm diameter and index of refraction n=1.49 was used in the experiments. The tube was enclosed in a plexiglas box filled with Potassium Thiocyanate and Ammonium Thiocyanate, combined in such a manner to achieve an index of refraction similar to the plexiglas. This would permit video taping the experiment and measuring the important dimensions from the video with little optical distortion. The fluid lining the tube walls, representing the thin film on the airway walls, is a silicone oil (Dow Corning 200 Fluid) with kinematic viscosity of 10^4 cSt and refractive index n=1.40. The core liquid, which models air, is a mixture of ethanol and water with a kinematic viscosity of 1.7 cSt. The ethanol and water mixture is prepared to match the specific gravity of the oil, which eliminates the affects of gravity from the experiment. The interfacial surface tension between the oil and ethanol, as measured by Otis[12] with a ring tensiometer, is 35 dynes/cm.

The pressure measurements were made using two Celesco transducers (model LCVR) with a full scale measurement of 0 to 10 cm H_2O. A C+ program (appendix B) and a LAB SE data acquisition board were used to record the data on a Mac. The LAB SE data acquisition board is an 8 bit analog-to-digital converter with a uniploar analog input range from 0 to 10 volts or bipolar input range of ±5 volts. The 0 to 10 volt range was used in these experiments.

Procedure. *Refer to figure 2.* The tube is completely filled with oil, and free of any trapped air bubbles. The upstream and downstream pressures are recorded before the experiment is started. These pressure measurements are an indication of the initial offset between the two transducers. The ethanol supply bath and sink are filled to a level which will determine the

---

[12]Otis, D.R., PhD thesis, Chapter 6, MIT, 1994

12

purge rate and plug velocity. The ethanol sink is filled to just about the level of the tube (x_3 x_2).

The section of the tube labeled A is removed and the valve is opened. The pressure gradient set up by the ethanol bath and sink drives the ethanol through the tube, leaving a thin film of oil on the tube walls. The rate the ethanol moves through the tube (called the 'purge rate') is regulated by the valve. The purge rate needs to be held constant for the duration of the purge in order obtain a uniform film.

Once the oil has been purged from the system, the valve is closed and a slug of oil is introduced by the syringe. The plug is allowed to settle until the menisci are axisymmetric. The valve is then opened and the slug translates down the tube. The velocity of the slug is set by the valve, and the pressures are recorded every second. The experiment is recorded on VHS tape and Global Lab Manager was used to capture still frames and digitize the data.
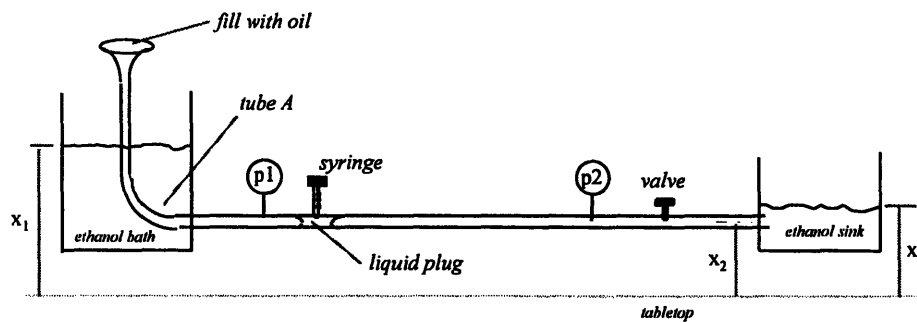

Figure 2. Test apparatus

Analytical

Dimensional Analysis. Dimensional analysis limits the number of experiments needed to characterize the slug behavior. The following dimensionless parameters were considered:

$$\dot{L}\frac{\mu}{\sigma} = f\left(\frac{\Delta p D}{\sigma}, \frac{D}{h_o}, \frac{D}{L_o} \right)$$

13

$$\frac{\mu V}{\sigma} = f\left(\frac{\Delta pD}{\sigma}, \frac{D}{h_o}, \frac{D}{L_o}\right)$$

$$\frac{h(t)}{D} = f\left(\frac{\Delta pD}{\sigma}, \frac{D}{h_o}, \frac{D}{L_o}\right)$$

In this way, the slug behavior is characterized by five dimensionless parameters instead of nine independent variables. It is characterized by five and not six because the plug velocity, film thickness and change in plug length are interdependent variables.

The dimensionless values were chosen to agree with what one might find in the respiratory bronchioles.

Parameter	Units	Respiratory Bronchioles	Experimental Value
D	cm	.05	1.24, .95
h_o	cm	.001	.03 - .09
σ	dyne-cm^{-1}	30	35
μ	dyne-sec-cm^{-2}	.01	100, 1
L_o	cm	?	1 - 5
Δp	cm H$_2$0	2 - 10	.2 to 1.5
$\dfrac{\Delta ph_o}{\sigma}$	-	.0001 to .0003	.0002 to .004
$\dfrac{D}{h_o}$	-	25 to 50	13 - 38
$\dfrac{\mu V}{\sigma}$	-	.003 x velocity	.1 to 2.4

Table 1. Physical parameters relevant to airway re-opening
(velocity in units of cm/s)

14

Conservation of Mass. The plug velocity, length and trailing edge film thickness are related through conservation of mass. Using the plug as the control volume, shown in figure 3, the following relationship is derived:

$$\frac{d}{dt}\int dVolume = -\int \overline{V} \bullet n \, dA$$

$$\frac{d}{dt}\left(\pi r^2 L(t)\right) = \pi(r^2 - s_o^2)V_L - \pi\left(r^2 - s^2(t)\right)V_t$$

$$\frac{dL}{dt} = \left(1 - \frac{s_o^2}{r^2}\right)V_L - \left(1 - \frac{s^2(t)}{r^2}\right)V_t \tag{1}$$

where V_L is the leading meniscus velocity, V_t is the trailing meniscus velocity, s_o is the initial film radius, $s(t)$ is the instantaneous film radius and dL/dt is the instantaneous change in plug length. The assumption is made that s_o is uniform along the length of the tube and does not change ahead of plug. It is also assumed that the volume of oil in the two end regions near the forward and aft menisci is relatively constant.
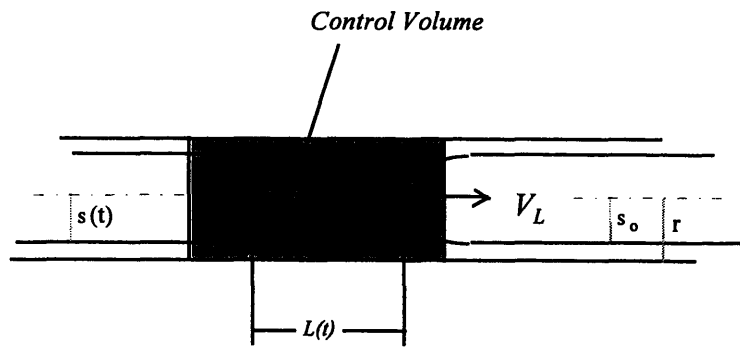
Control Volume

Figure 3. Control volume of the liquid bridge

The plug velocity Vp is taken to be the average of the leading meniscus velocity (V_L) and the trailing meniscus velocity (V_t).

$$V_p = \frac{V_i + V_L}{2}$$

(2)

Film Deposition. G.I. Taylor and Bretherton quantified the fraction of a viscous fluid (m) deposited on a tube wall when expelled by a low viscosity fluid as a function of capillary number. Taylor plotted his experimental results as shown in figure 4:
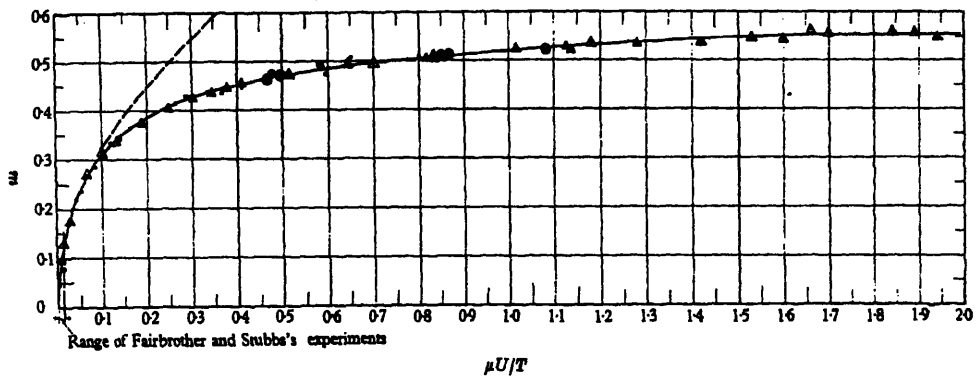
Figure 4. Fraction of fluid deposited on tube wall
copied from reference 7. G.I. Taylor's experimental results.

Bretherton derived an empiracal equation to predict the the fraction of film deposited (eq 3) on the tube wall:

$$W = 1.29\left(3\frac{\mu V}{\sigma}\right)^{\frac{2}{3}}$$

(3)

Bretherton and Taylor's results can be used to predict the trailing film thickness by replotting the data as film thickness versus capillary number.as shown in figure 5.

16
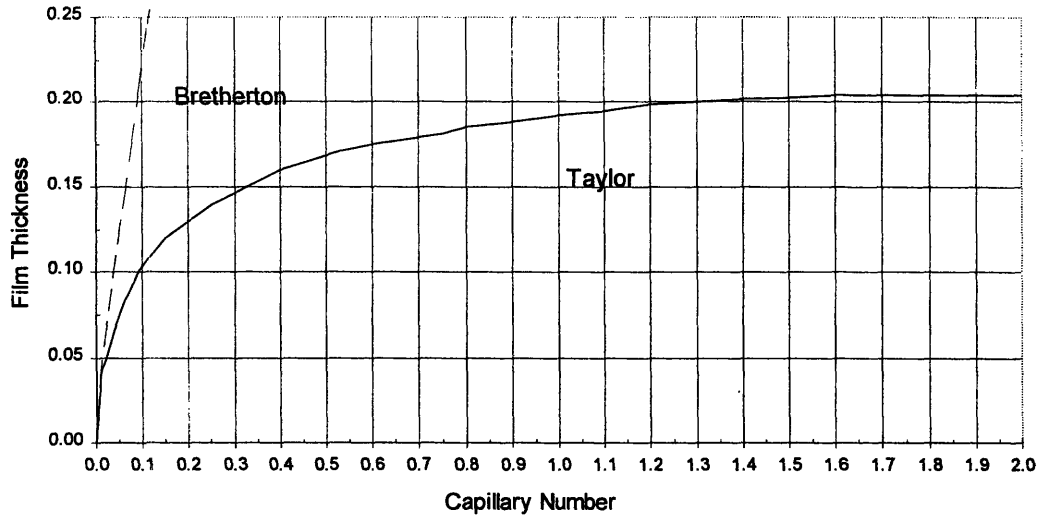
Figure 5. Bretherton and Taylor's results plotted as film thickness (r=.62)

The fraction of the viscous fluid deposited on the tube wall 'm' (or 'W' by Bretherton) is defined as:

$$m = \frac{U - U_m}{U}$$

where U is the velocity of the meniscus at the fluid interface and U_m is the average mean velocity of the viscous fluid. Referring to the control volume shown in figure 6, the film thickness, h, is calculated as:

$$\pi\left(R^2 - s^2\right)U = \pi R^2\left(U - U_m\right)$$

$$\frac{U - U_m}{U} = \frac{R^2 - s^2}{R^2} = m$$

$$s = \sqrt{R^2 - mR^2} = R\sqrt{1 - m}$$

$$h = R - s \tag{4}$$

17
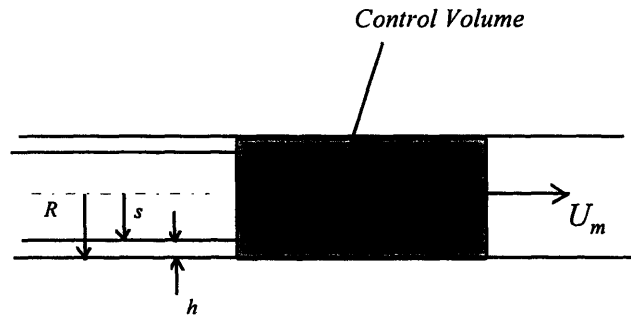
Figure 6. Control volume to calculate film thickness in Taylor's experiments

Using equations 3 and 4, Bretherton's and Taylor's results are plotted as film thickness vs. capillary number (R=.62 cm) as shown in figure 5.

Data Reduction

Index of Refraction. The dimensional data (L(t), h(t) and velocities) were measured using Global Lab Manager. Still frames were captured from the video tape, digitized and measured directly. The film thickness measurements were corrected for the difference in the index of refraction between the plexiglas and oil. It is assumed that the index of refraction of the $NH_4CSN/KSCN$ solution matches the index of the plexiglas.
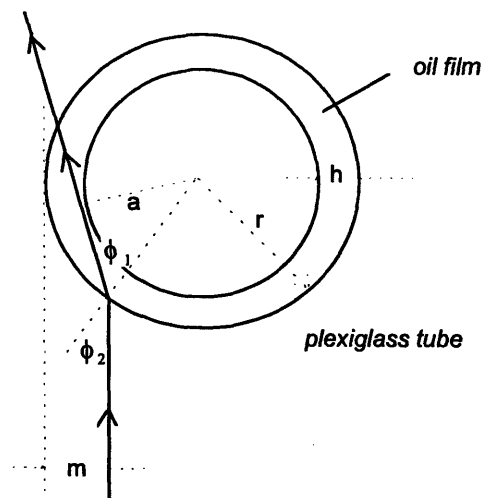
Figure 7. Optical Correction for Film Thickness

$$\sin\phi_2 = \frac{r-m}{r}$$

$$\sin\phi_1 = \frac{a}{r}$$

$$n_1 \sin\phi_1 = n_2 \sin\phi_2$$

$$\sin\phi_1 = \frac{n_2}{n_1}\frac{r-m}{r} = \frac{a}{r}$$

$$a = \frac{n_2}{n_1}(r-m)$$

$$h = r - a = r - \frac{n_2}{n_1}(r-m) \tag{5}$$

'h' is the true film thickness, 'm' is apparent film thickness measured from the video tape, and 'r' is the tube radius. The index of refraction for the oil is n1=1.40 oil and the index of refraction for the plexiglas is n2=1.49.

Pressure Correction for Curvature: The transducers measure the pressure within the oil film on the tube wall. The pressure gradient across the meniscus is the difference in the ethanol pressure. Therefore, to determine the ethanol pressure the oil pressure needs to be corrected for curvature and surface tension:
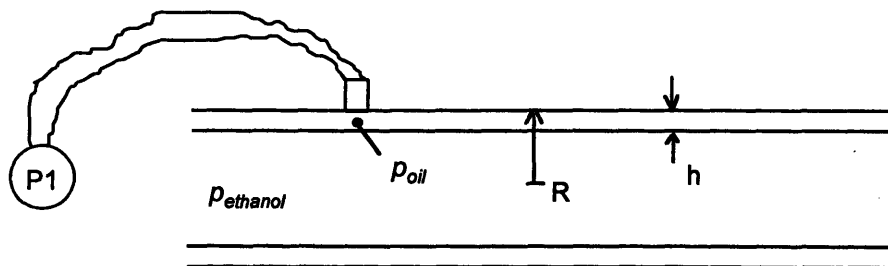
Figure 8. Pressure correction for curvature and surface tension

p1 is the measured pressure in the oil film, or poil. If the film thickness is constant at both transducers than this correction is ot necessary to determine the pressure difference across the meniscus.

$$P_{ethanol} = P_{oil} + \frac{\sigma}{R}$$

Chapter 3

Results

The objective of these experiments is to identify a relationship between the pressure drop across the plug, the plug velocity, the deposited film thickness and the plug dissipation rate. The experimental results were grouped by initial film thickness (D/h_o) and initial plug length (D/L_o) to identify possible correlations to the initial conditions. The results are non-dimensionalized as discussed in the "methods" section and plotted as a function of capillary number. The raw data is located in appendix A. The results will be presented in the following order:

- *Non-dimensional Pressure vs. Capillary Number.* A discussion on the viscous and capillary pressure contributions to the total pressure drop across the plug is included. The results show that the viscous contribution is significant.

- *Plug Dissipation vs. Capillary Number.* The results will show that faster moving plugs dissolve faster with the initial film thickness having a secondary influence on the plug velocity.

• *Comparison of Film Thickness to Predictions.* The assumptions used in the conservation of mass equations are reasonable and predict film thickness fairly well. The measured film thickness is essentially independent of capillary number and therefore the results of Taylor and Bretherton, which are very dependent on capillary number, are not in agreement.

Pressure Contributions. A plot of the non-dimensional pressure vs. capillary number is shown in figure 9.
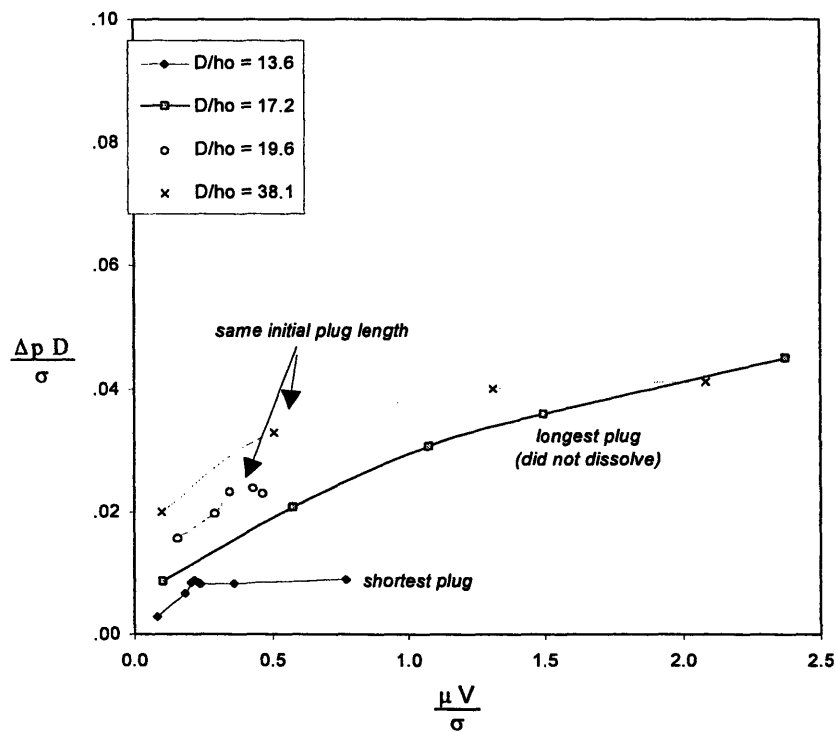

Figure 9. Non-dimensional pressure vs. capillary number

As the plug travels along the tube, the pressure drop across the plug stabilizes but the velocity continues to increase until the meniscus breaks. The exception to this is the longest

plug, in which case the meniscus never broke and the pressure drop continued to rise. In each case, the pressure stabilizes when the viscous pressure drop becomes small compared to the pressure drop associated with the surface tension at the meniscus. In the case of the very long plug, the viscous stress never becomes small and in fact continues to increase as the plug begins to dissolve.

The total pressure drop across the plug is a summation of the pressure required to overcome the viscous stress which develops when the plug is displaced by the ethanol and the difference in capillary pressure drop across the two menisci at the ethanol/oil interfaces.

$$P_{total} = P_{vis} + P_{cap} \tag{6}$$

The viscous and capillary pressure drops are approximated as

$$P_{vis} = \frac{8\pi\mu V_p L}{A} + P_{end}$$

$$P_{cap} = \frac{\sigma}{R}\bigg|_{trailing} - \frac{\sigma}{R}\bigg|_{leading} \tag{7}$$

where Vp is the plug velocity, L is the length of the plug, A is the flow area and R is the menisci radii (trailing meniscsus and leading meniscus). (Because the meniscus radii are difficult to measure, the difference in capillary pressure is taken to be the measured total pressure minus the viscous pressure.)

Figure 10 shows the viscous pressure contribution to the total pressure for two of the four cases of figure 9. The remaining pressure contribution comes from the pressure drop across the meniscus due to surface tension (referred to as the capillary pressure). The two sets of data shown in figure 10 were chosen because they have the same initial plug length but

22

different initial film thicknesses. (Following will be a discussion for two cases with the same initial film thickness but different initial plug lengths.) As shown in figure 10, the viscous pressure rises to a peak becoming the major contributor to the total pressure, then drops off abruptly. At this point the total pressure stabilizes and the meniscus continues to increase in velocity. As the plug translates down the tube, the meniscus changes from an axisymmetric to a bullet-like shape. (see figure 11). This decrease in meniscus radius increases the capillary pressure drop which eventually becomes the dominant contributor to the total pressure drop.
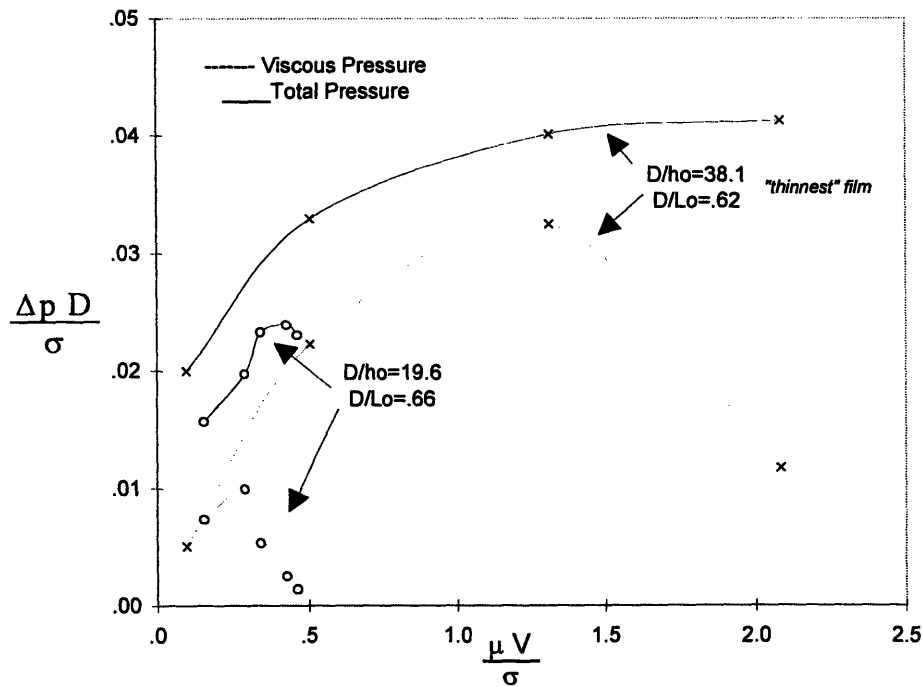
Figure 10. Viscous pressure contribution to the total pressure for plugs with the same initial length

(the solid line is the total measured pressure drop, the shaded line is the viscous pressure as calculated by equation 7. The viscous contribution drops off as the pressure stabilizes)

The total pressure is higher for the plug with the thinner film (x). Both plugs start with approximately the same viscous stress, but the asymmetry between the menisci becomes more prevalent in the plug with the thinner film. Therefore, there is a greater capilllary

pressure contribution.   In addition, the viscous stress in the plug with the thinner film increases as the plug travels, increasing its total pressure. The plug with the thinner film is actually traveling faster than the plug with the thicker film. (see table 2) As a result, the viscous stress increases. These results suggest the initial film thickness influences the plug velocity.

Figure 11. Bullet Shape of Trailing Meniscus
(trailing meniscus radius is small, capillary pressure is high)

	D/ho=19.6 (o)				D/ho=381. (×) *(thinnest film)*		
time	*Vplug*	*Length*	$\frac{\Delta p_{vis}D}{\sigma}$	*time*	*Vplug*	*Length*	$\frac{\Delta p_{vis}D}{\sigma}$
41	0	1.878	0	30	0	2.003	0
49	.05	1.793	.0074	65	.03	1.884	.0051
69	.10	1.253	.0100	81	.18	1.603	.0223
90	.12	.569	.0054	86	.46	.903	.0325
100	.15	.216	.0025	88	.73	.206	.0118
105	.16	.112	.0014				

Table 2. Plug Velocity and Length of Two Plugs Starting With Same Initial Length
(the thinner film plug (x) travels faster but decreases in length slower. As a result, the viscous stress is larger- see equation 7)

Figure 12 compares the pressure contributions between two plugs that start off with approximately the same film thickness, but different initial plug lengths. The pressure in the very the long plug (□) is all viscous. In fact the viscous pressure drop is greater than the total pressure drop across the plug. This is possible because the leading meniscus inverts as shown in figure 13. The pressure across the leading meniscus *decreases* thus balancing the total pressure drop across the plug. The viscous stress in the short plug (♦) drops off soon after it begins to move and the pressure stabilizes. The long plug is so long that the viscous stress continues to rise and the pressure nevers stabilizes.
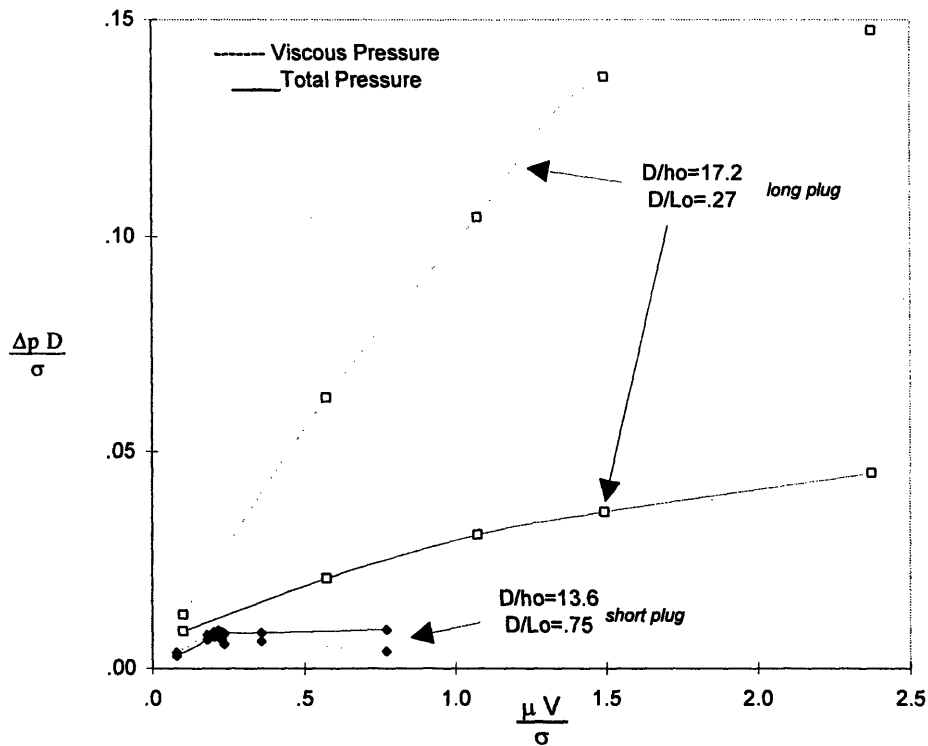
Figure 12. Viscous pressure drop compared to the total pressure drop
for plugs with the same initial film thickness
(the solid line is the total measured pressuredrop, the shaded line is the viscous pressure drop as calculated by equation 3.)
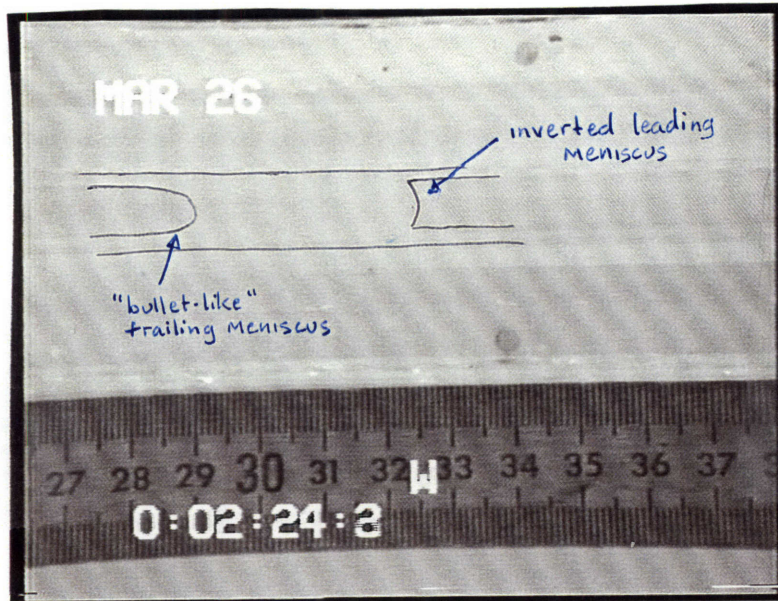
Figure 13. Leading meniscus inverts decreasing the pressure drop across the plug

Plug Dissipation. The average rate the plug decreases in length as a function of the average capillary number is shown in figure 14. The faster moving plugs dissolve faster; shorter plugs travel faster than the longer plugs. In addition, the initial film thickness seems to have a secondary affect. The thinner films travel faster than the thicker films.
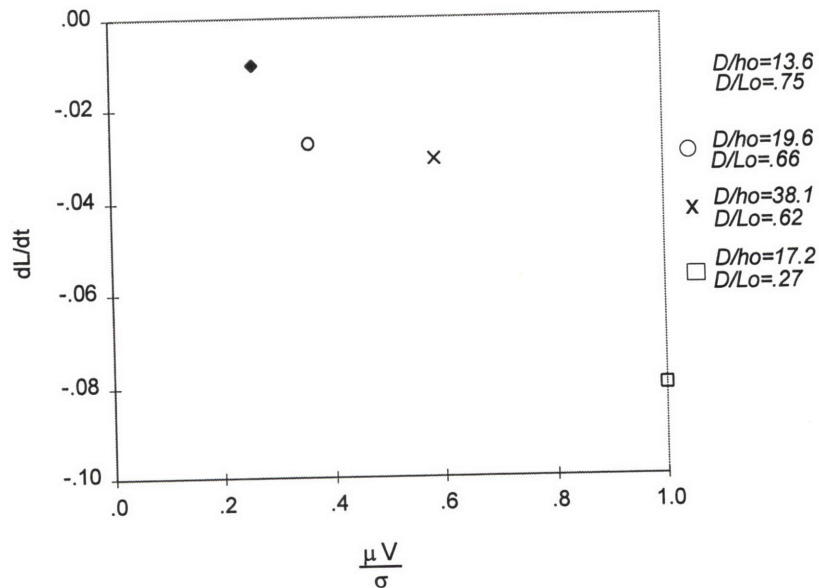
Figure 14. Average rate a plug decreases in length increases with capillary number

The instantaneous change in plug length is shown in figure 15 as a function of the instantaneous capillary number and in figure 16 as a function of non-dimensional pressure. (The plug is considered to have dissolved once the plug becomes very thin. In some cases a thin, flat meniscus would not completely break but continue to flow through the tube.).
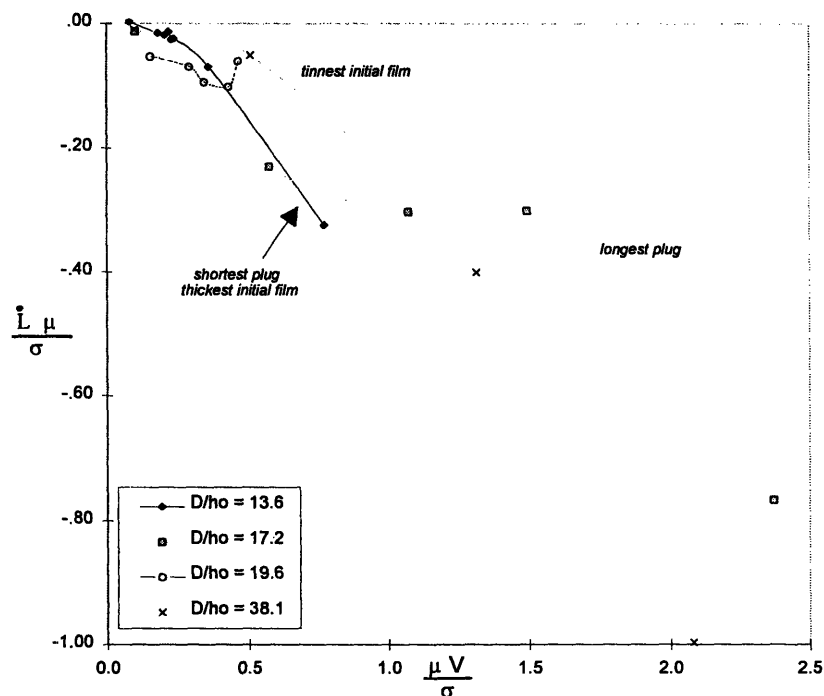
Figure 15. Plug dissolves faster with increasing capillary number

Figure 16 suggests a relationship between the plug dissipation rate, the pressure drop and initial film thickness - to achieve the same rate of dissipation, the plugs with the thinner films require greater pressures. This is somewhat redundant to figures 14 & 15 because, as was discussed, faster moving plugs dissolve faster; and faster moving plugs experience a greater pressure drop. Also, it was seen in figure 14 that the initial film thickness does influence on the pluge velocity.

Figure 16

Y-axis: $\dfrac{\overset{\bullet}{L}\,\mu}{\sigma}$ with values .00, -.20, -.40, -.60, -.80, -1.00

X-axis: $\dfrac{\Delta p\,D}{\sigma}$ with values .00, .01, .02, .03, .04, .05

shortest plug

longest plug

Legend:
- D/ho = 13.6
- D/ho = 17.2
- D/ho = 19.6
- D/ho = 38.1
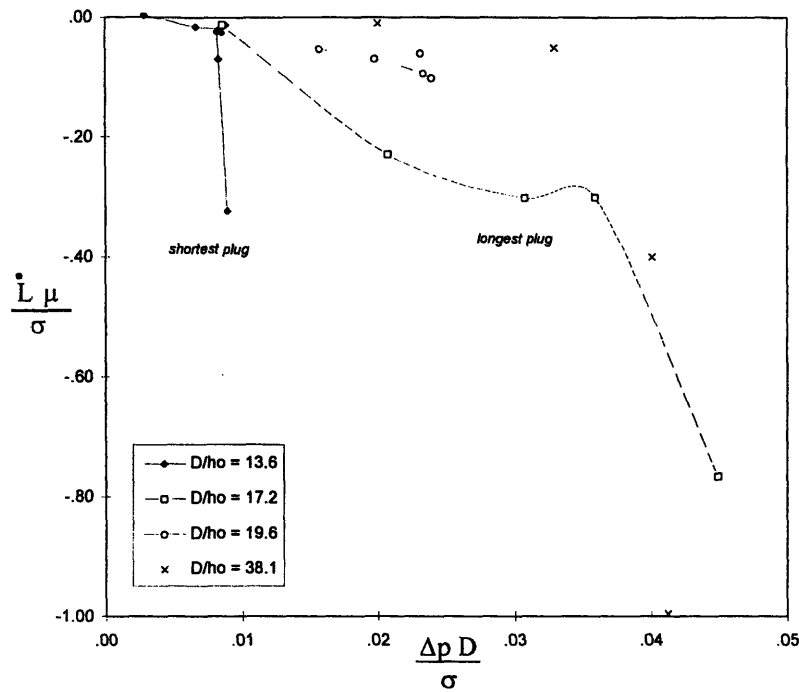
Figure 16. Rate of dissipation increases with pressure drop across the plug
(thinner films experience greater pressure drops)

Comparison With Predictions of Trailing Film Thickness

Conservation of Mass. Figure 17 shows a comparison of the calculated film thickness using conservation of mass (eq 1) and the measured film thickness. There is fair agreement. Except for a few scattered points, the measured data ranges from ~.06 to .10 cm and the calculated values vary from .08 to .12 cm. There are three possible reasons for the discrepancies. (1) The resolution in the film thickness measuring technique was not fine enough. The error in the measurement would be on the order of a pixel. Because the magnifcation of the experiments was not consistent from experiment to experiment, the length of a pixel will vary for each experiment. But, one can estimate the error to be about .02 cm. (2) The index of refraction between the plexiglass and $NH_4CSN/KSCN$ solution was not matched. This would introduce an error in the calculating the corrected film thickness (eq 5) (3) The error introduced in calculating the film thickness from conservation of mass

due the errors in measuring the initial film thickness, the plug velocity and dL/dt, or in the assumption that the volume of oil around the menisci remains constant.

Film Thickness Based on Conservation of Mass
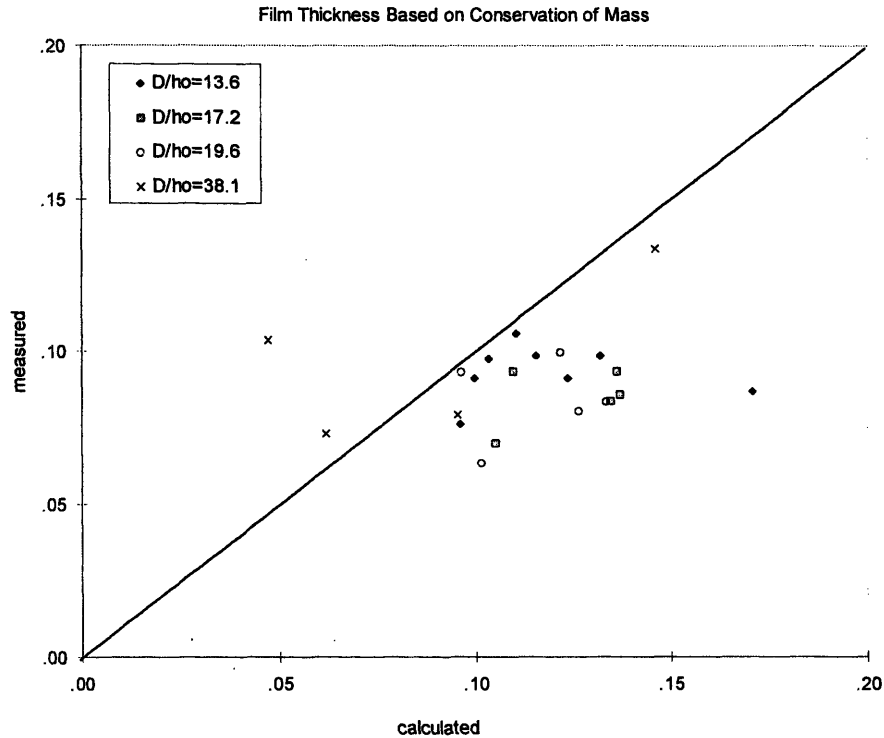
Figure 17. Comparison of calculated film thickness using conservation of mass to the measured film thickness.
(conservation of mass overpredicts the film thickness)

Film Deposition. A comparison of the film thickness calculated using Taylor and Bretherton's results to measured film thicknesses is shown in figure 18. The capillary number does not influence the deposited film thickness except perhaps at low capillary numbers. The film thickness is relatively constant (avg=.09 cm, std. dev. = .015cm). The measured values deviate significantly from Bretherton's because Bretherton derived his results for capillary numbers lower than the experimental. Bretherton conducted his experiments at Ca~10^{-3}; these experiments were at Ca~.1 to 2.4.
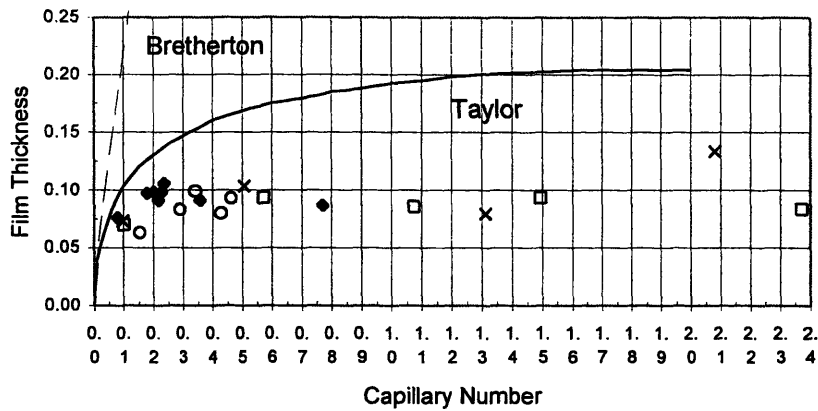
Figure 18. Comparison of measured and calculated film thickness using Taylor and
Bretherton's results

(film thickness is not a function of capillary number, except perhaps at very low capillary numbers)

A comparison between the two methods of calculating the film thickness (Taylor and conservation of mass) is shown in figure 19. Conservation of mass consistently underpredicts Taylor.
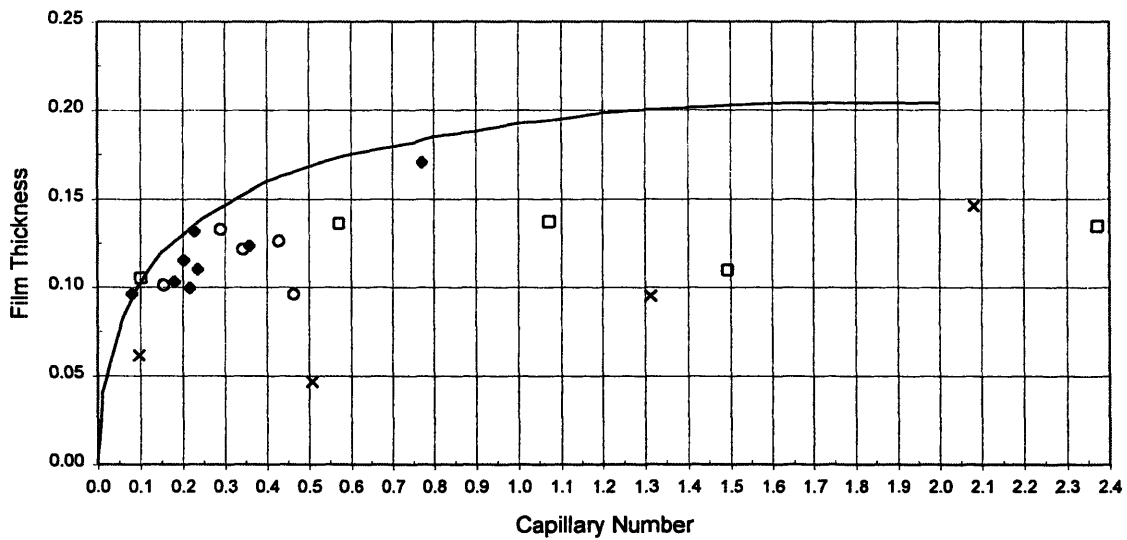
Figure 19. Comparison of film thickness as calculated by conservation of mass and Taylor

30

Chapter 4

Discussion

Influence of initial film thickness. Gaver found that the initial film thickness within the region of the collapsed tube did not affect the re-opening times of collpased airways. In the case of a liquid plug however, the inital film layer does play a role. This can be explained using conservation of mass. Equation 1 has been rewritten to show the plug velocity dependency on initial film thickness. It is approximated that $V_p \approx V_l \approx V_t$.

$$\frac{V_p}{r^2} = \frac{dL/dt}{s^2(t) - s_o^2} \tag{8}$$

Gaver's situation (an inviscid fluid displacing a viscous fluid, and forcing the collpased walls apart) can be modeled using the control volume of figure 5 and conservation of mass.

$$\frac{V_p}{r^2} = \frac{U_m}{s^2(t)} \tag{9}$$

This is equation 4 is rewritten in a similar manner to equation 8 where V_p is the meniscus velocity noted as U in equation 4. One can see the influence of the initial film thickness plug velocity in equation 8. If the initial film is thick such that $s_o \rightarrow 0$, then equations 8 and 9

become the same, where dL/dt is analogous to the mean velocity of viscous fluid (U_m) in Gaver's experiments. For a small initial layer, $s_0 \to r$ and the plug velocity (Vp) is greater as was shown in the experiments (figure 14). The plugs with the thinner initial films ($\times$) traveled faster than the plugs with the thicker initial films ($\blacklozenge$). This is an important consideration during surfactant replacement therapy. Depending on the initial layer lining the airway walls, the slug of surfactant may travel quickly and completely dissolve before reaching the outer branches of the bronchial tree, or it may travel slowly through the tree depositing very little along its journey.

Pressure drop across a liquid plug. The total pressure drop across the plug has two components - the pressure needed to overcome the viscous stress which develops in the plug and the pressure needed to overcome the surface tension forces at the menisci.

$$\Delta P_{total} \approx P_{cap} + P_{vis} + P_{cap}$$

$$\Delta P_{total} \approx \frac{\sigma}{R_1} + \frac{8\pi\mu V_p L}{A} - \frac{\sigma}{R_2}$$
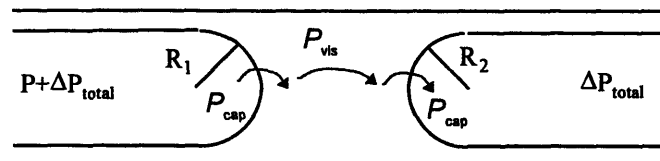

Figure 20. Pressure drop across liquid plug

Initially, the total pressure is comprised primarily of the viscous stress. However, as the plug travels the menisci take on the shapes shown in figure 21. In this condition, R1 decreases

32

and R2 increases The total pressure drop becomes dominated by the pressure required to

jump the trailing meniscus.
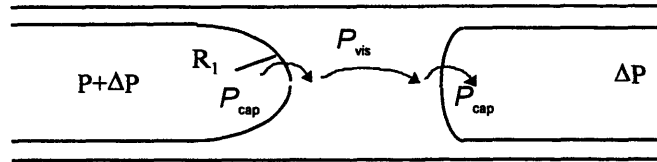
Figure 21. Menisci shape and pressure drop changes across liquid plug

For small capillary numbers, Gaver found similiar results, i.e, the surface forces dominated

and the pressure required to move the meniscus is determined by the pressure jump across

the meniscus. Gaver found the minimum pressure required to re-open a collapsed airway to

be $\sim 8\sigma/R$. As explained by Gaver, this implies that the flexible tube permits the radius of the

meniscus to become $\sim 1/8$ of the tube radius. In the idealized model of a liquid plug in a rigid

tube, the meniscus radius can not get that small and no minimum threshold pressure was

found. If a minimum pressure did exist it would be $\sim \sigma/R$, or .06 cm H_2O. The experiments

were not conducted at pressure drops this low.

Gaver plotted his non-dimensional opening pressures vs the capillary number and found the

data collapsed onto a single line (figure 22). In contrast, the liquid plug has a family of

curves correlated to initial film thickness. For easy reference figure 9 is re-plotted. Figure 9

falls well below Gaver's results. Gaver's situation requires greater opening pressures

because the capillary pressure is always significant (only one meniscus) where as in the rigid

tube model, the capillary pressure can tend towards zero if the menisci are symmetric. In

addition, the family of curves was seen in the rigid tube experiments because the asymmetry

between the menisci becomes significant with smaller initial film thicknesses.

33
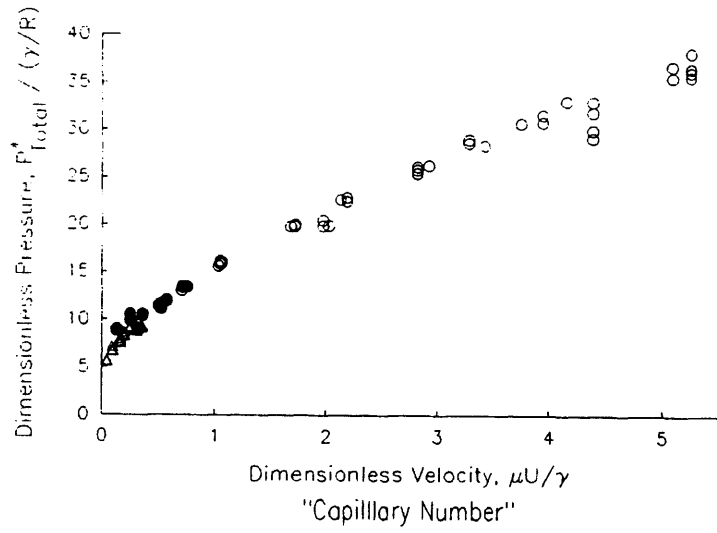
Figure 22. Gaver's plot of non-dimensional pressure vs. capillary number
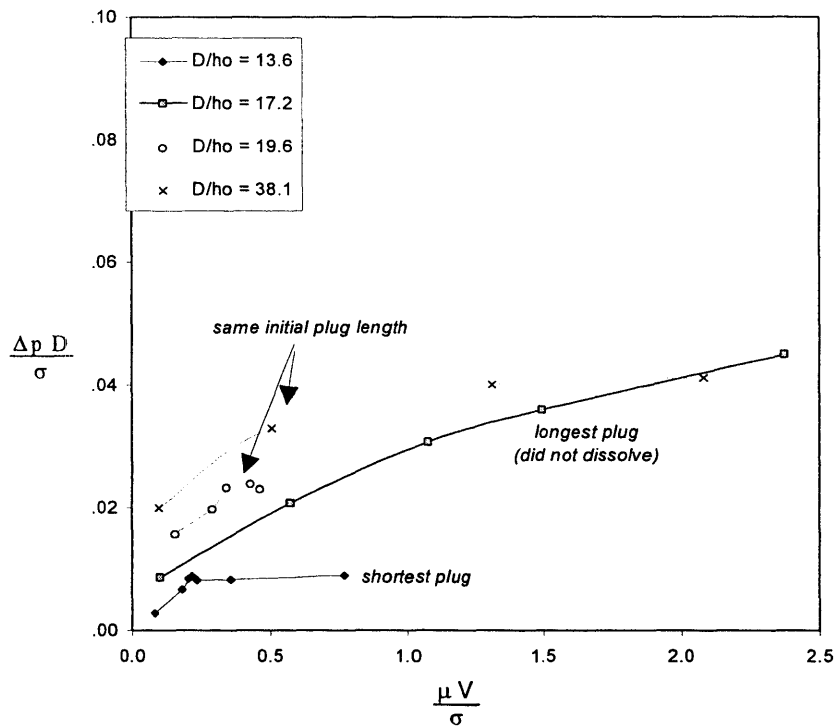
Figure 9. Non-dimensional pressure vs. capillary number

Airway re-opening is believed to be a rapid occurrence. This was inferred from the stepwise drop in impedance measured by Otis from an excised canine lung. He observed an increase in impedance during expiration which indicated a closure had occurred. During inspiration, the impedance would instantaneously drop which was presumed to be the airway re-opening. The experiments completed do not indicate that a stepwise drop in impedance would be detected when the meniscus breaks. As the meniscus nears disentegraton, the pressure has stabilized.

Liu also experienced an immediate drop in pressure when forcing a liquid plug through a narrow section of tube. He presumed this to be analogous to an airway re-opening during inspiration. However, unlike the behavior of a liquid plug which "shrinks" over time, Liu's column of liquid did not shrink, but squeezed through the restricted region and then "popped" out the other side. This implies that the rapid drop Otis measured could be the "popping" open of a collapsed air way or a liquid plug being squeezed through a constricted region of an airway. Either case, the meniscus dissolving does not explain the drop in impedance measurements.

Conclusions

The following conslusions are drawn from the experiments:

1. The deposited film thickness seems constant.

2. Therefore, the faster moving plugs lose volume more rapidly (larger dL/dt).

3. The total pressure drop is much less than the total pressure seen by Gaver due to the two menisci offseting each other and reducing the capillary pressure contribution.

4. The viscous pressure is a significant contributor to the total pressure. The capillary pressure drop is also significant because of the asymmetry of the menisci at the fluid interfaces.

35

Appendix A. Experimental Data

(diagram) p1 · p2 · oil (liquid plug) · ethanol · ethanol · L(t) · D · h_0 · $h_1(t)$ · $\mu,\ \sigma$
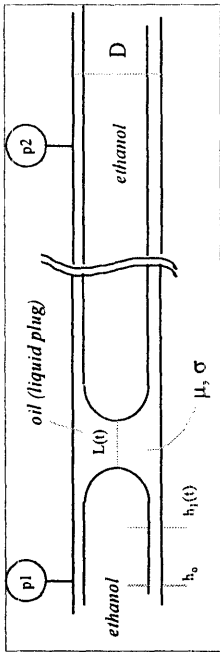
Experiment #5

n_oil	1.40	index of refraction
n_plexi	1.49	index of refraction
D	1.24	cm
μ	100	dyne-sec/cm^2
σ	35	dyne/cm
ρ	0.96	g/cm^3
Lo	1.66	cm
ho_mea	.123	cm
ho_act	.091	cm
D/ho	13.6	
D/Lo	.75	
ist. trav	13.8	cm
time	154	sec
avg Vp	.09	cm/s
$\frac{\mu V}{\sigma}$	.26	avg

*valve opens at 20 seconds

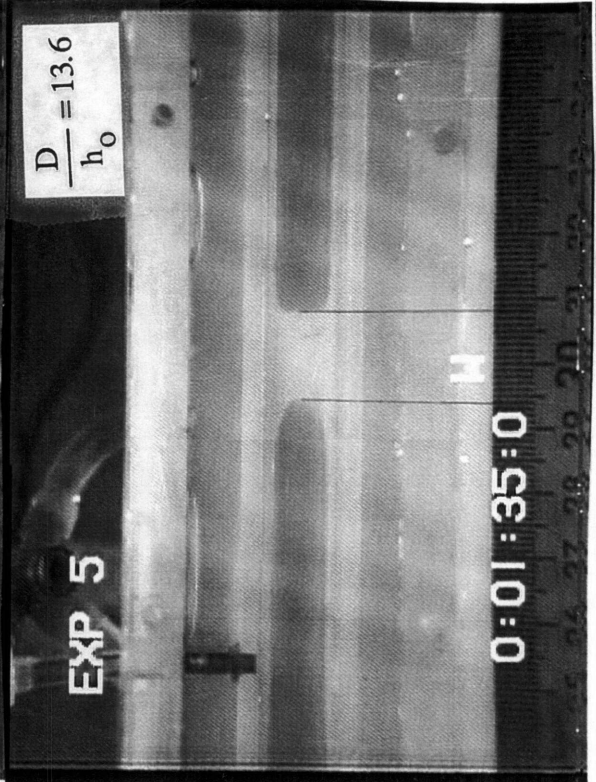| time sec	L cm	dL/dt cm/s	Vt cm/s	VL cm/s	Vp cm/s	mean Vp cm/s	h1_meas cm	h1_act cm	$\Delta h(t)$ cm	p1_meas cm H2O	p2_meas cm H2O	p1_act cm H2O	p2_act cm H2O	Δp cm H2O	$\overline{\Delta p}$ cm H2O	$\overline{\Delta p}_{vis}$ cm H2O	$\frac{\Delta p\, D}{\sigma}$	$\frac{\Delta p_{vis} D}{\sigma}$	$\frac{\mu V}{\sigma}$	$\frac{\dot{L}\,\mu}{\sigma}$	h(t)/D	L(t)/D
0	1.660						.123	.091	.000	6.33	6.32	72.5	72.5	.01								
35	1.677	.001	.05	.06	.06	.03	.109	.076	-.015	6.28	6.13	72.4	72.3	.16	.08	.10	.0029	.0037	.08	.003	.061	1.35
55	1.572	-.005	.08	.07	.07	.06	.129	.097	.006	6.23	6.01	72.4	72.2	.22	.19	.22	.0067	.0078	.18	-.015	.079	1.27
95	1.319	-.006	.08	.07	.07	.07	.130	.099	.007	6.17	5.92	72.3	72.1	.25	.24	.21	.0084	.0074	.20	-.018	.079	1.06
120	1.214	-.004	.08	.08	.08	.08	.123	.091	.000	6.17	5.93	72.3	72.1	.25	.25	.20	.0089	.0072	.22	-.012	.073	.98
135	1.084	-.009	.08	.08	.08	.08	.130	.099	.007	6.20	5.94	72.3	72.1	.24	.24	.19	.0086	.0068	.23	-.025	.079	.87
160	.881	-.008	.09	.08	.09	.08	.137	.106	.015	6.21	5.97	72.4	72.1	.23	.23	.16	.0082	.0057	.24	-.023	.085	.71
170	.642	-.024	.18	.15	.17	.13	.123	.091	.000	6.21	5.96	72.4	72.1	.25	.24	.18	.0083	.0063	.36	-.068	.073	.52
174	.189	-.113	.43	.33	.38	.27	.119	.087	-.004		5.95	72.4	72.1	.26	.25	.11	.0090	.0040	.77	-.324	.070	.15

EXP 5 $\dfrac{D}{h_o} = 13.6$ 0:00:35:0

EXP 5 $\dfrac{D}{h_o} = 13.6$ 0:01:35:0

EXP 5 $\dfrac{D}{h_o} = 13.6$ 0:00:00:0

EXP 5 $\dfrac{D}{h_o} = 13.6$ 0:00:55:0

Figure (schematic): labels — p1, p2, ethanol, oil (liquid plug), ethanol, L(t), D, h_o, $h_i(t)$, μ, σ
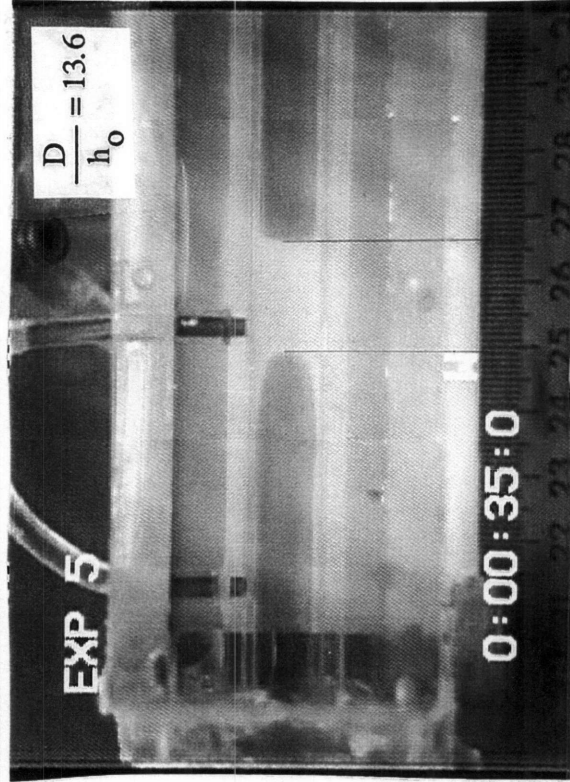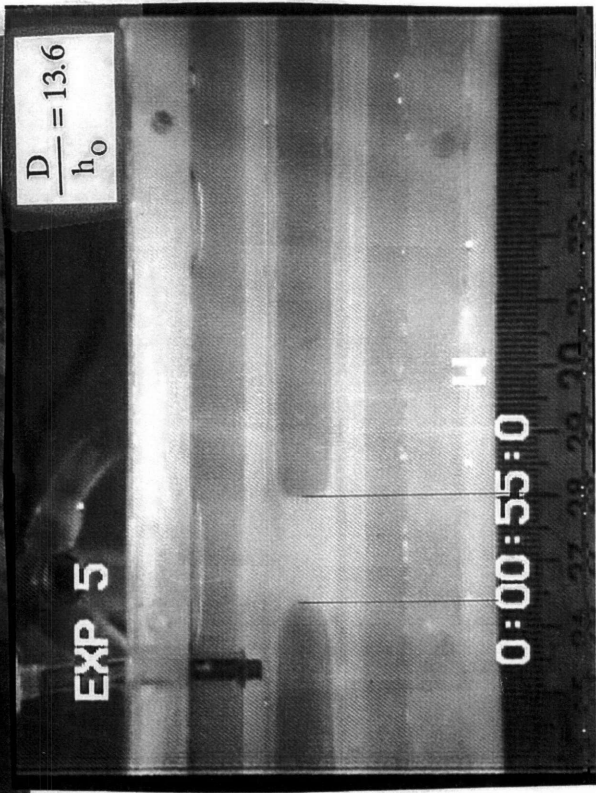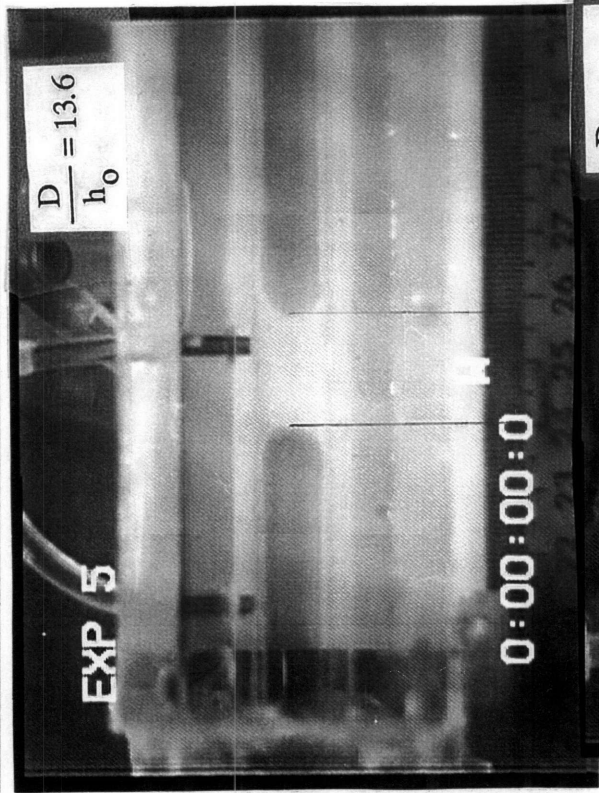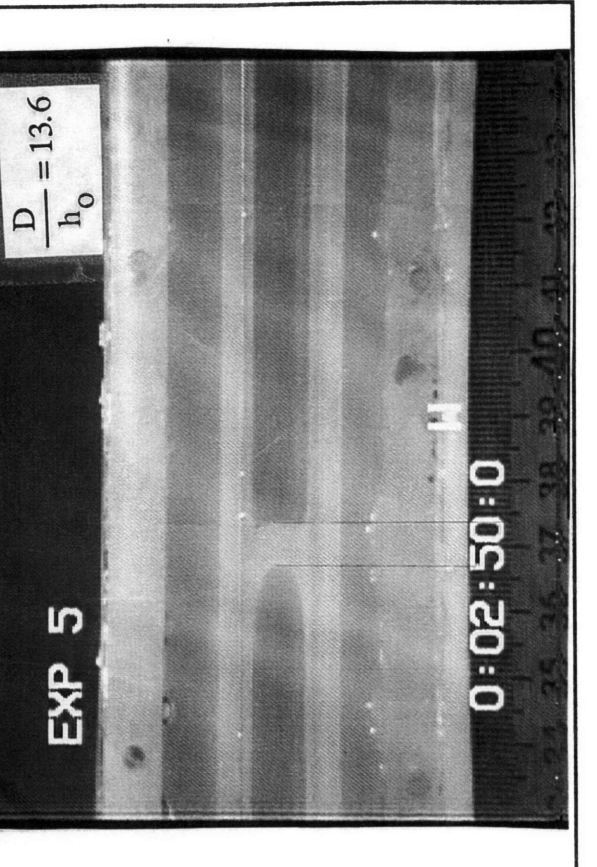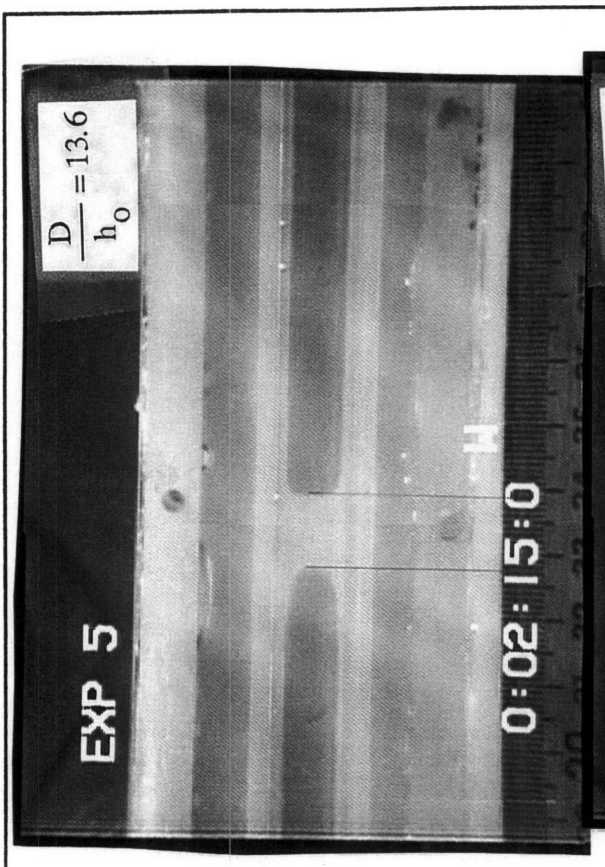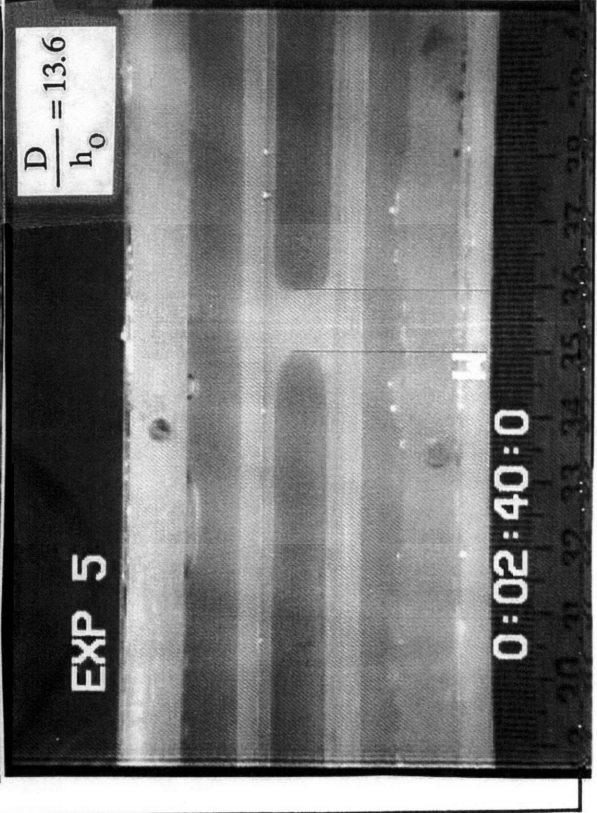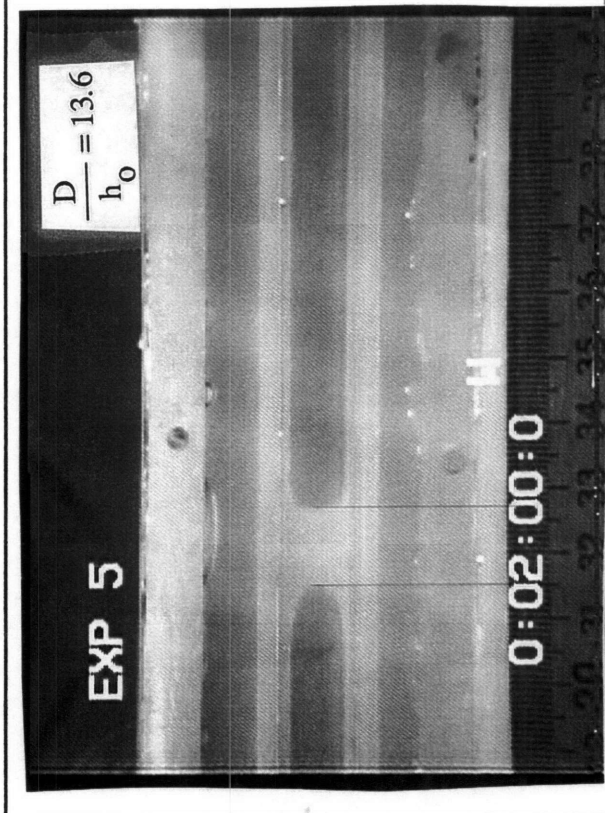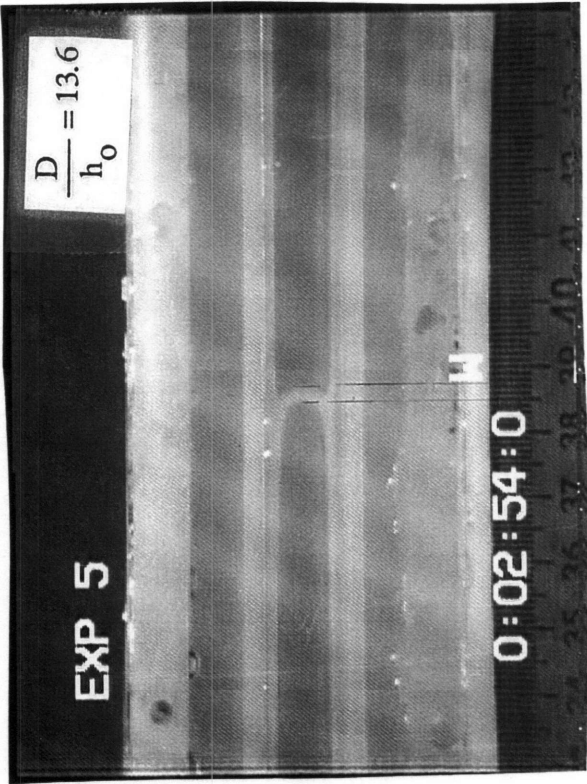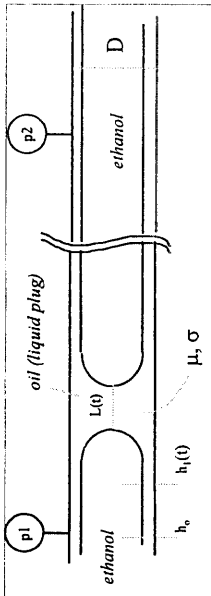
March 26 - Experiment #1

n_oil	1.40	index of refraction
n_plexi	1.49	index of refraction
D	1.24	cm
μ	100	dyne-sec/cm^2
σ	35	dyne/cm
ρ	.96	g/cm^3
Lo	4.514	cm
ho_meas	.105	cm
ho_act	.072	cm
D / ho	17.2	
D/Lo	.27	
dist. travel	10.0	cm
time	29	sec
avg Vp	.35	cm/s
$\dfrac{\mu V}{\sigma}$	1.00	avg

*valve opens at 120 seconds

time sec	L cm	dL/dt cm/s	Vt cm/s	VL cm/s	Vp cm/s	mean Vp cm/s	h1_meas cm	h1_act cm	Δh(t) cm	p1_meas cm H2O	p2_meas cm H2O	p1_act cm H2O	p2_act cm H2O	Δp cm H2O	$\overline{\Delta p}$ cm H2O	$\overline{\Delta p}_{vis}$ cm H2O	$\dfrac{\Delta p\,D}{\sigma}$	$\dfrac{\Delta p_{vis}\,D}{\sigma}$	$\dfrac{\mu V}{\sigma}$	$\dfrac{L\,\mu}{\sigma}$	h(t)/D	L(t)/D
120	4.514						.107	.074	.002	6.32	6.23	70.18	70.08	.10								
132	4.461	-.004	.07	.08	.07	.04	.103	.070	-.002	6.32	5.93	70.18	69.79	.39	.24	.35	.0086	.0124	.10	-.013	.056	3.60
138	3.978	-.081	.37	.29	.33	.20	.125	.093	.021	6.31	5.52	70.16	69.38	.78	.59	1.76	.0207	.0625	.57	-.230	.075	3.21
142	3.554	-.106	.47	.37	.42	.38	.118	.086	.014	6.31	5.35	70.16	69.20	.96	.87	2.95	.0308	.1045	1.07	-.303	.069	2.87
144	3.343	-.106	.70	.55	.63	.52	.125	.093	.021	6.31	5.23	70.16	69.09	1.07	1.02	3.86	.0360	.1369	1.49	-.301	.075	2.70
148	2.270	-.268	1.19	.88	1.04	.83	.116	.084	.012	6.31	4.84	70.16	68.70	1.46	1.27	4.16	.0450	.1475	2.37	-.766	.067	1.83

Diagram labels: p1, p2, oil (liquid plug), ethanol, ethanol, D, $L(t)$, h_o, $h_1(t)$, μ, σ
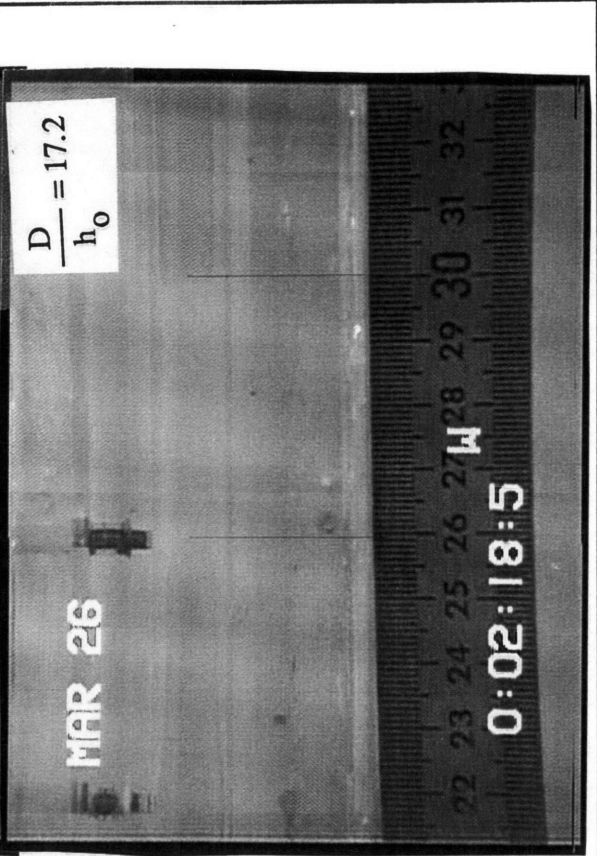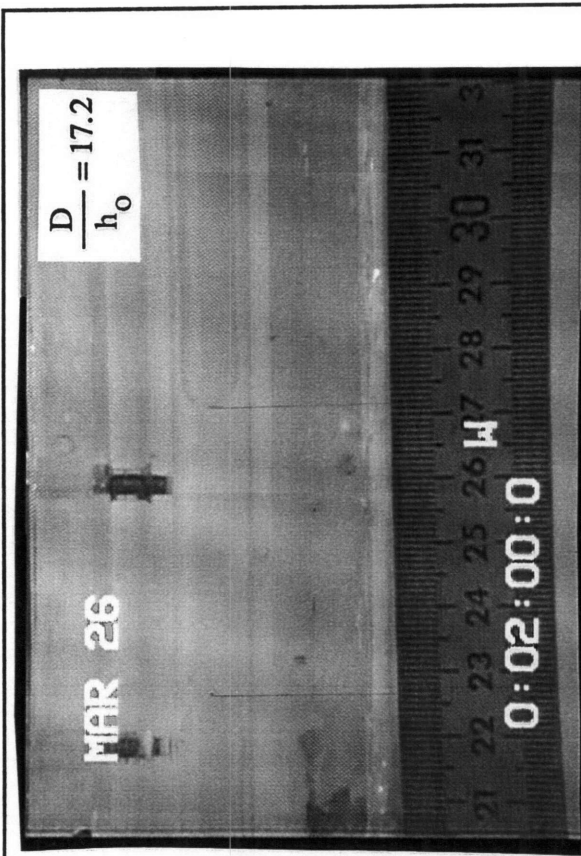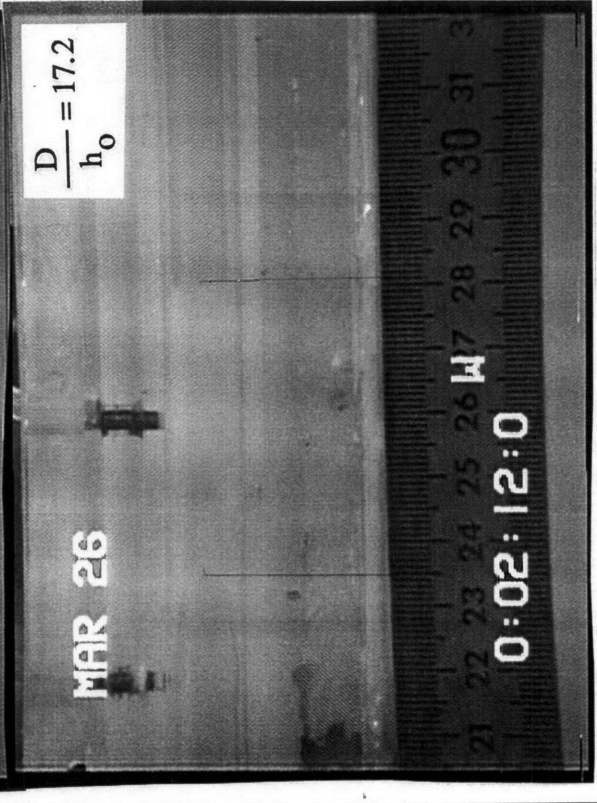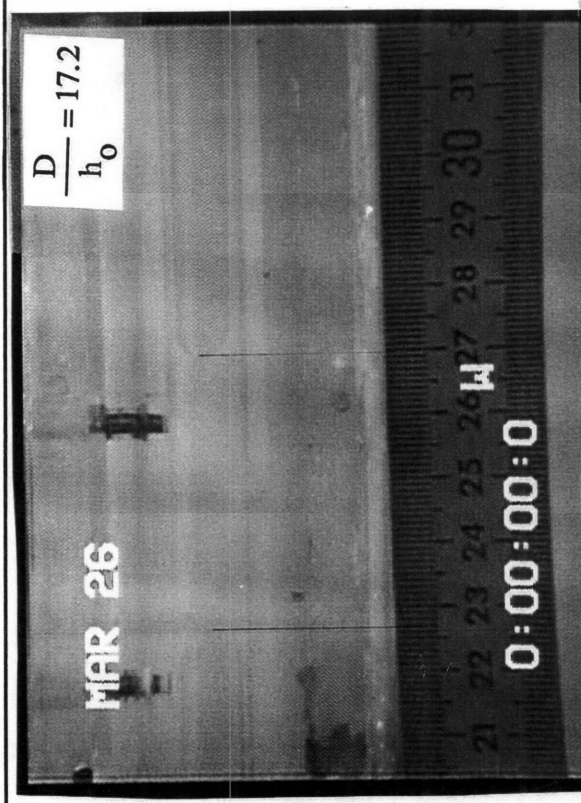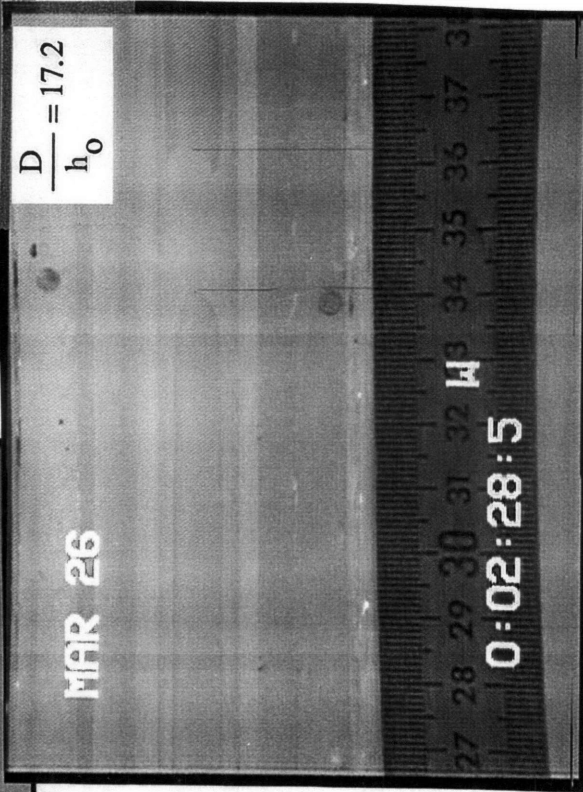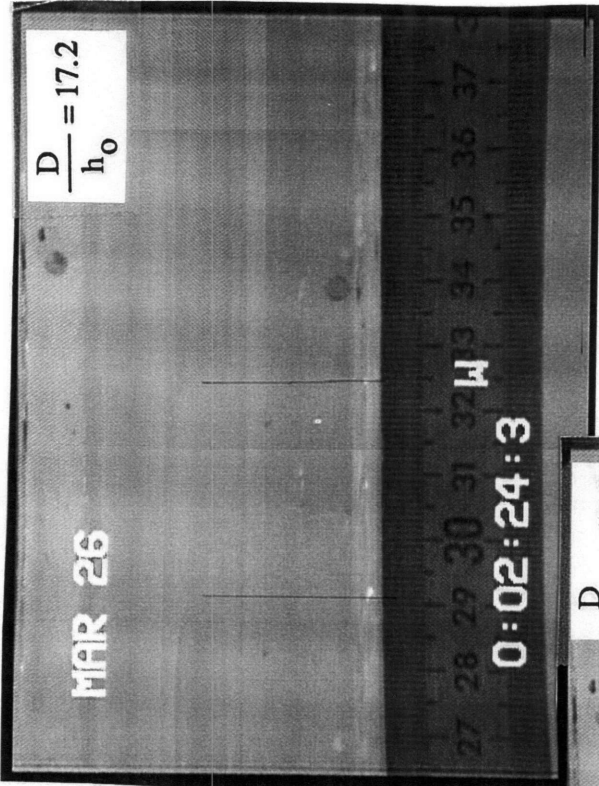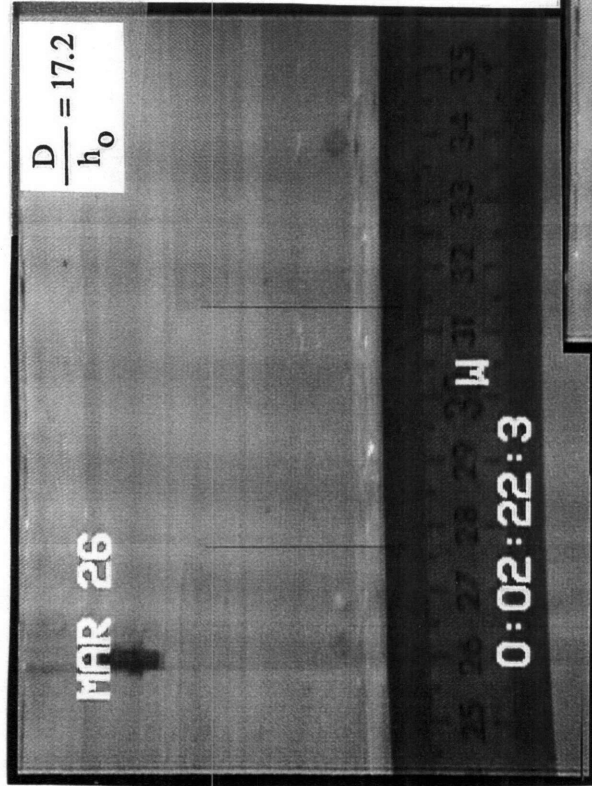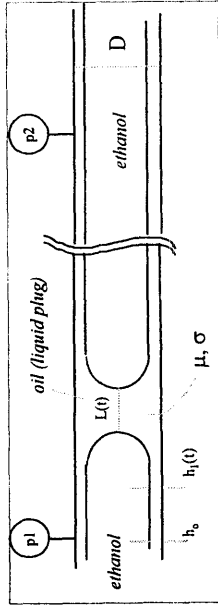
Jan. 21 - Experiment #1

n_oil	1.40	index of refraction
n_plexi	1.49	index of refraction
D	1.24	cm
μ	100	dyne-sec/cm^2
σ	35	dyne/cm
ρ	.96	g/cm^3
Lo	1.878	cm
ho_meas	.097	cm
ho_act	.063	cm
D / ho	19.6	cm
D/Lo	.66	
dist. travel	8.1	cm
time	65	sec
avg Vp	.12	cm/s
$\frac{\mu V}{\sigma}$	.36	avg

*valve opens at 40 seconds

time sec	L cm	dL/dt cm/s	Vt cm/s	VL cm/s	Vp cm/s	mean Vp cm/s	h1_meas cm	h1_act cm	Δh(t) cm	p1_meas cm H2O	p2_meas cm H2O	p1_act cm H2O	p2_act cm H2O	Δp cm H2O	$\overline{\Delta p}$ cm H2O	$\overline{\Delta p}_{vis}$ cm H2O	$\frac{\Delta p\,D}{\sigma}$	$\frac{\Delta p_{vis}\,D}{\sigma}$	$\frac{\mu V}{\sigma}$	$\frac{\dot{L}\,\mu}{\sigma}$	h(t)/D	L(t)/D
0	1.878						.097	.063	.000	4.70	4.28	67.6	67.2	.42								
41	1.878						.078	.043	-.020	4.67	4.27	67.5	67.1	.40								
49	1.731	-.018	.12	.10	.11	.05	.097	.063	.000	4.67	4.18	67.5	67.1	.49	.44	.21	.0157	.0074	.16	-.052	.051	1.40
69	1.253	-.024	.11	.09	.10	.10	.116	.084	.020	4.67	4.04	67.5	66.9	.63	.56	.28	.0198	.0100	.29	-.068	.067	1.01
90	.569	-.033	.16	.13	.15	.12	.131	.100	.036	4.67	3.98	67.5	66.9	.69	.66	.15	.0233	.0054	.34	-.093	.080	.46
100	.216	-.035	.17	.14	.16	.15	.113	.080	.017	4.66	4.00	67.5	66.9	.66	.68	.07	.0239	.0025	.43	-.101	.065	.17
105	.112	-.021	.18	.16	.17	.16	.125	.093	.030	4.65	4.01	67.5	66.9	.64	.65	.04	.0231	.0014	.46	-.059	.075	.09
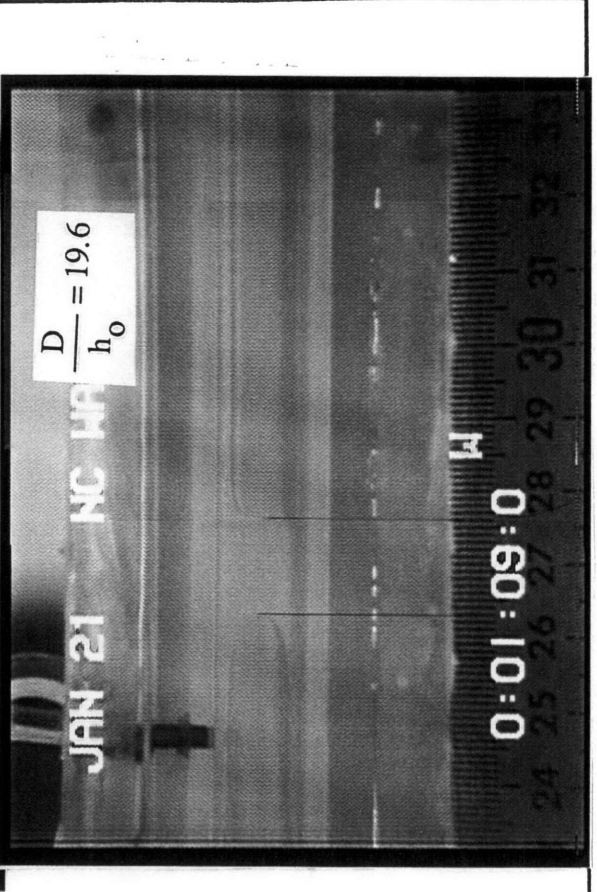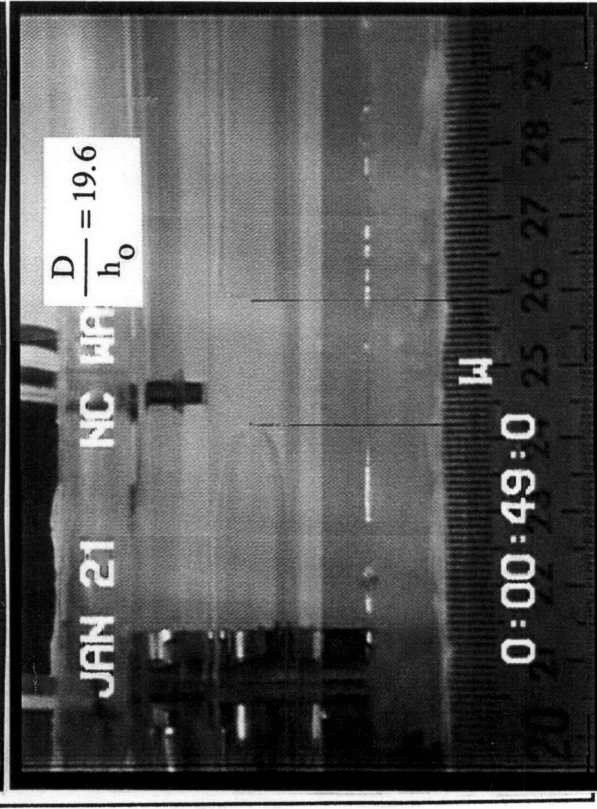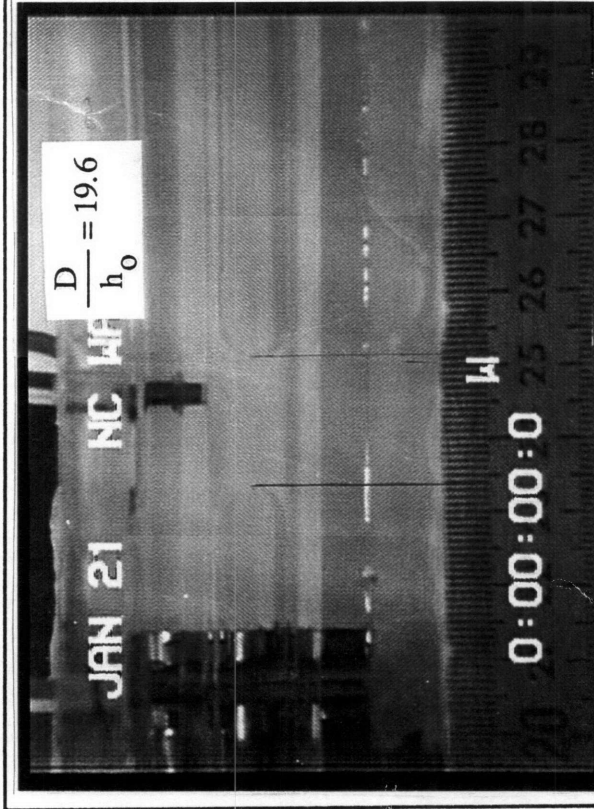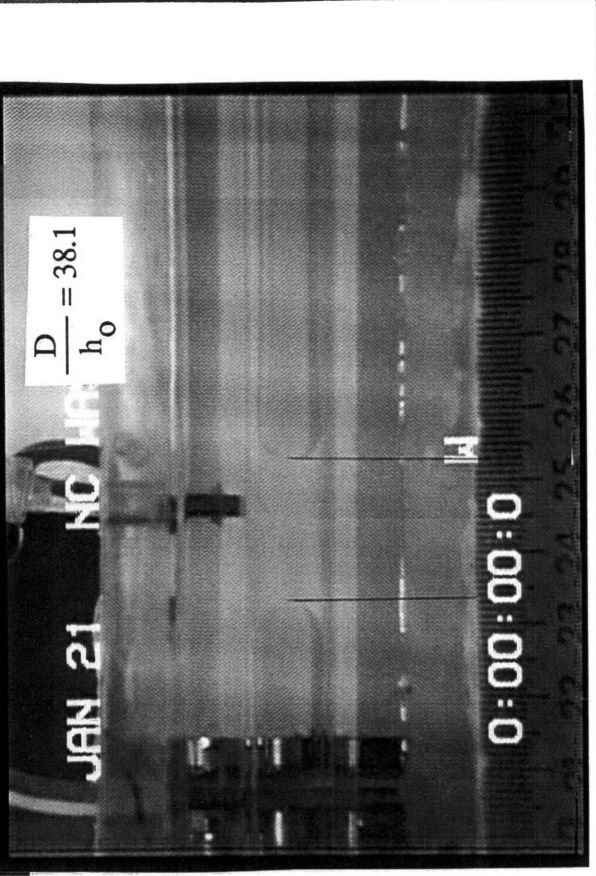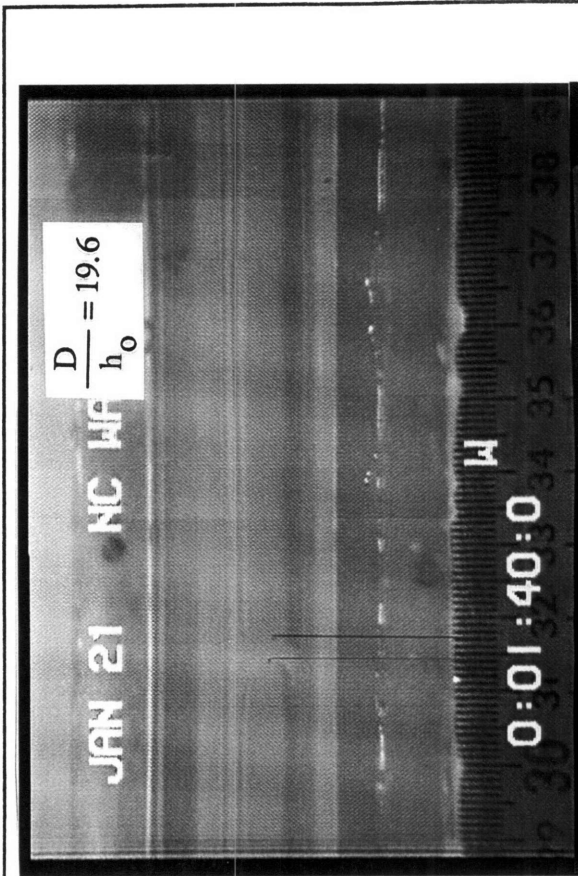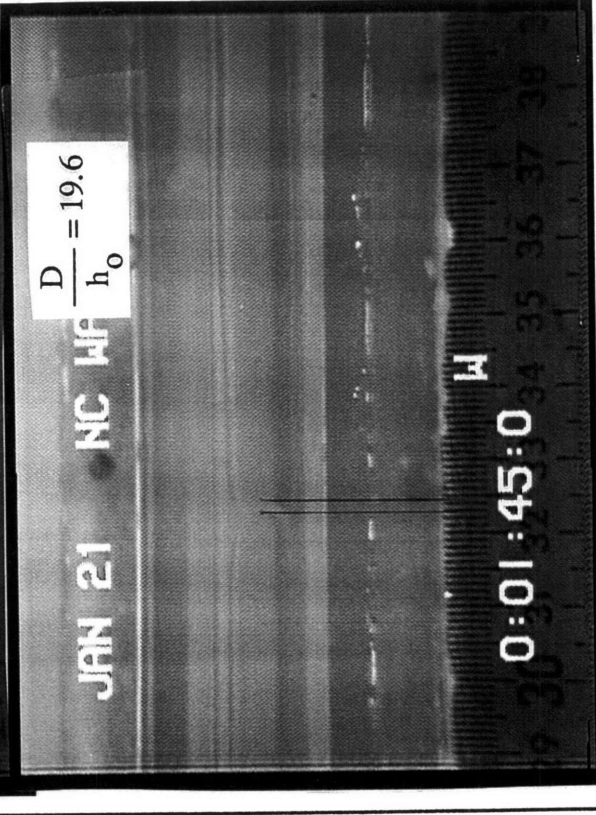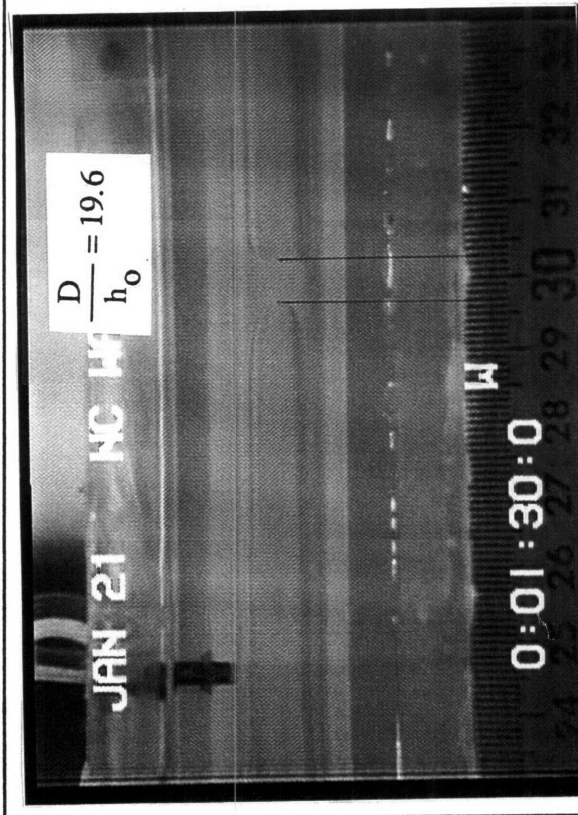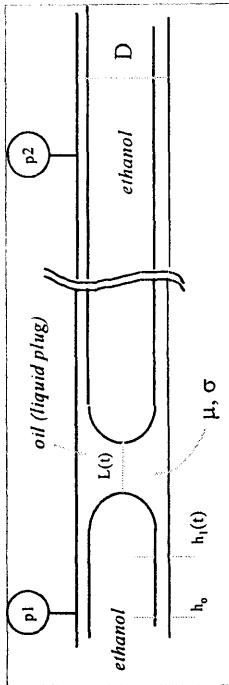
Jan. 21 - Experiment #2

n_oil	1.40	index of refraction
n_plexi	1.49	index of refraction
D	1.24	cm
μ	100	dyne-sec/cm^2
σ	35	dyne/cm
ρ	.96	g/cm^3
Lo	2.003	cm
ho_meas	.068	cm
ho_act	.033	cm
D / ho	38.1	
D/Lo	.62	
dist. travel	12	cm
time	58	sec
avg Vp	.21	cm/s
$\dfrac{\mu V}{\sigma}$	.59	avg

* valve opens at 30 seconds

time	L	dL/dt	Vt	VL	Vp	mean Vp	h1_meas	h1_act	$\Delta h(t)$	p1_meas	p2_meas	p1_act	p2_act	Δp	$\Delta \bar{p}$	$\Delta \bar{p}_{vis}$	$\dfrac{\Delta p\, D}{\sigma}$	$\dfrac{\Delta p_{vis} D}{\sigma}$	$\dfrac{\mu V}{\sigma}$	$\dfrac{\dot{L}\,\mu}{\sigma}$
sec	cm	cm/s	cm/s	cm/s	cm/s	cm/s	cm	cm	cm	cm H2O	cm H2O	cm H2O	cm H2O	cm H2O	cm H2O	cm H2O				
0	2.003						.068	.033	.000	4.68	4.31	64.26	63.88	.38						
65	1.884	-.003	.06	.08	.07	.03	.106	.073	.040	4.60	3.85	64.18	63.43	.75	.57	.14	.0200	.0051	.10	-.010
81	1.603	-.018	.31	.27	.29	.18	.135	.104	.071	4.54	3.43	64.11	63.01	1.11	.93	.63	.0329	.0223	.51	-.050
86	0.903	-.140	.70	.57	.63	.46	.112	.079	.047	4.54	3.38	64.11	62.96	1.16	1.13	.92	.0401	.0325	1.31	-.400
88	0.206	-.349	1.00	.65	.83	.73	.163	.134	.101	4.54	3.37	64.11	62.94	1.17	1.16	.33	.0413	.0118	2.08	-.996

47
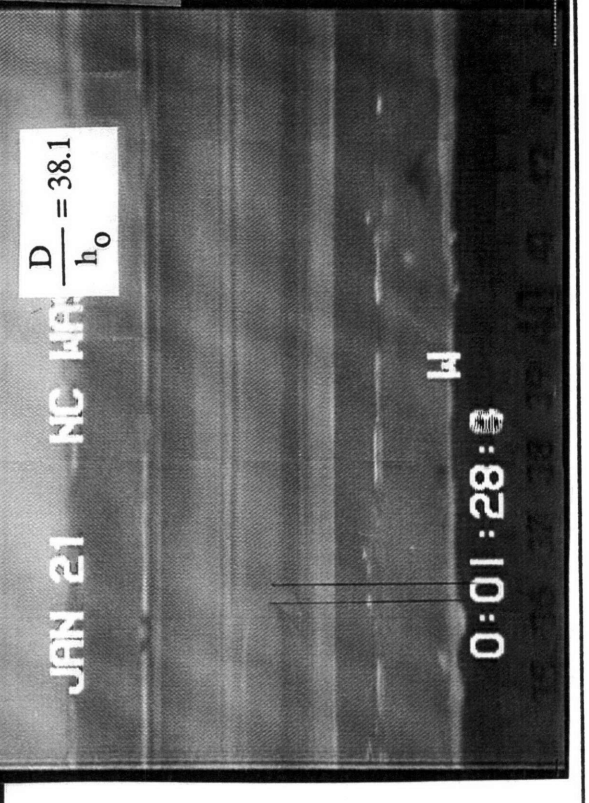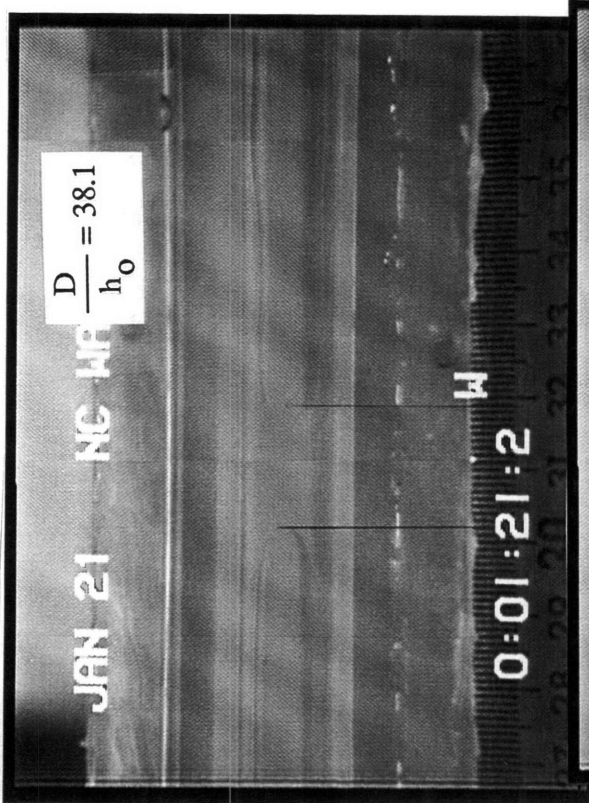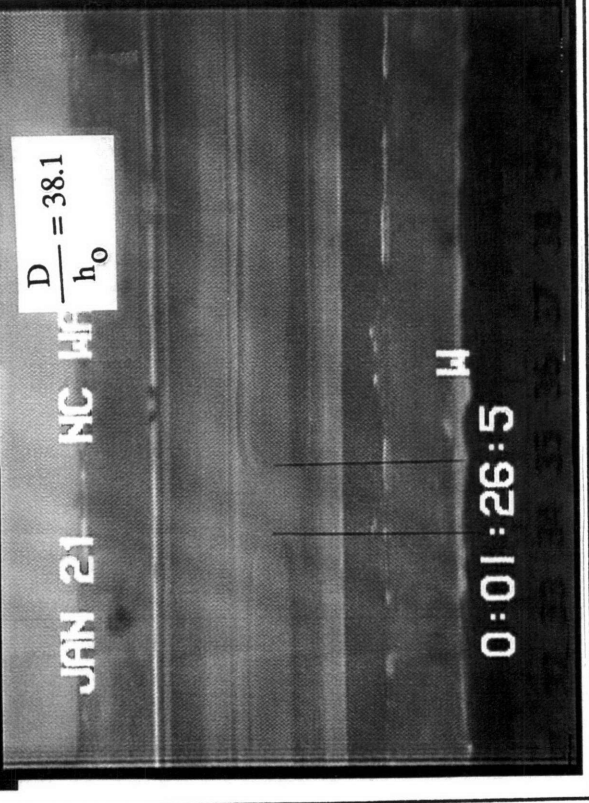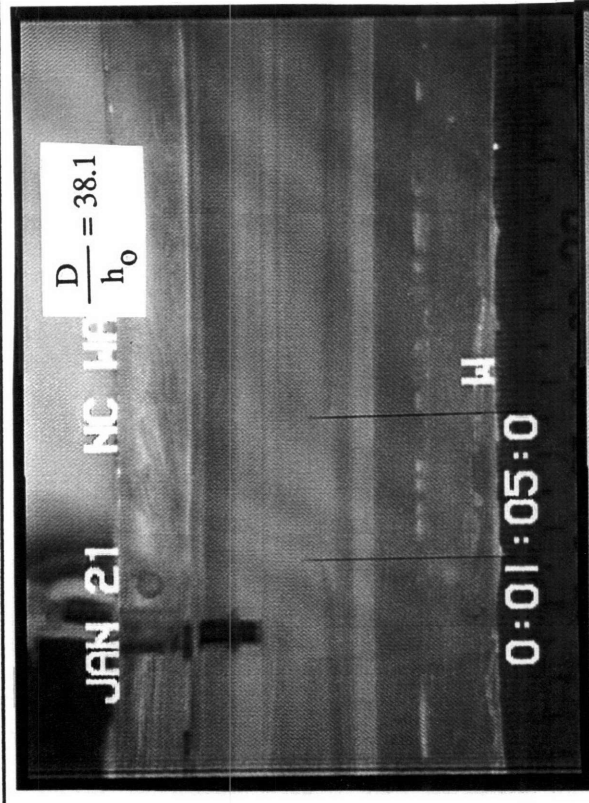
Appendix B. Data Acquisition Program

```c
/*
 * 2ChDataAcq.c  -  This program acquires data on 2 channels on the LAB-SE
 *                  board using LabSE LabDriver interface routines.
 */

typedef short int int16;
typedef long  int int32;

extern int16 LDSysError;                /* global system error code */


#include <stdio.h>
#include <stdlib.h>
#include <console.h>
#include <unix.h>


#define    COUNT 4L                      /* Total number of samples to acquire */
#define NUM_CHANS 2                      /* scan 2 channels */

main()
{
              int16 slot, channel, timebase, error, error1, status;
              int16 gain, chan, *ptr_array[16], samp_no, read_interval, elap_time;
              int16 input_mode, input_range, polarity;
              int16 i, k;
              char *buffer, *chanlAdata, *chanlBdata, outfile[20];
              int32 samp_interval, CountperChanl;
              float *volt_arrayA, *volt_arrayB;
              FILE *fp;

/* NULL the acquisition buffer pointers */
              buffer = NULL;
              chanlAdata = NULL;
              chanlBdata = NULL;
              volt_arrayA = NULL;
              volt_arrayB = NULL;

/* set up window used by the stdio routines */
              console_options.top = 45;
              console_options.ncols = 100;
              console_options.nrows = 14;
              console_options.title = (unsigned char*)"\p2chDataAcq";

/* open output file to store voltage readings */
              printf ("Input the name of the output file\n");
```

```c
        scanf("%s",outfile);
        fp = fopen(outfile,"w");

/* acquire memory for acquisition buffers */
        if ((buffer = (char *) calloc(COUNT,1L)) == NULL)          /* allocate 4 integers */
                {
                printf("\nMemory Allocation Err");
                return(-1);
                }


        CountperChanl = COUNT / NUM_CHANS;

        if ((chanlAdata = (char *) calloc(CountperChanl,1L)) == NULL) /* allocate 2 ints */
                {
                printf("\nMemory Allocation Err");
                if (buffer != NULL) free (buffer);
                return(-1);
                }
        if ((chanlBdata = (char *) calloc(CountperChanl,1L)) == NULL) /* allocate 2 ints */
                {
                printf("\nMemory Allocation Err");
                if (buffer != NULL) free (buffer);
                if (chanlAdata != NULL) free (chanlAdata);
                return(-1);
                }
        if ((volt_arrayA =(float *) calloc(CountperChanl,4L)) == NULL) /* allocate 2 floats */
                {
                printf("\nMemory Allocation Err");
                if (buffer != NULL) free (buffer);
                if (chanlAdata != NULL) free (chanlAdata);
                if (chanlBdata != NULL) free (chanlBdata);
                return(-1);
                }
        if ((volt_arrayB =(float *) calloc(CountperChanl,4L)) == NULL)   /* allocate 2 floats */
                {
                printf("\nMemory Allocation Err");
                if (buffer != NULL) free (buffer);
                if (chanlAdata != NULL) free (chanlAdata);
                if (chanlBdata != NULL) free (chanlBdata);
                if (volt_arrayA != NULL) free (volt_arrayA);
                return(-1);
                }

        slot = 0;
        gain = 1;
        timebase = 1;                   /* timebase = 1 ==> 1μs timebase */
```

```
                samp_interval = 25L;    /* sampling rate = 1 /( samp_interval * timebase) */

/* timebase = 1, samp_interval = 25L ==> Sampling rate = 40KHz */

/* configure for unipolar voltage range from 0 to 10 volts; polarity =1 */
/* configure for bipolar voltage range from -5 to +4.96 volts; polarity = 0 */

                error = AI_Config(slot,input_mode=0, input_range=10, polarity=1);

/* begin data acquistion */
                printf("\n How many seconds between pressure readings? \n");
                scanf("%d",&read_interval);

                printf("\n Time \t Channel 0 \t Channel 1");
                fprintf(fp,"\n Time \t Channel 0 \t Channel 1");

                elap_time=0;
                samp_no = 1;
                for (k=0; k < 200; k++)
                {
                /* start scanning data */
                error=Lab_SCAN_Start(slot,NUM_CHANS,gain,buffer,CountperChanl,
                                timebase,samp_interval);
                chkerr("Lab_SCAN_Start", error);
                if (error)
                                {
                                error = DAQ_Clear(slot);
                                chkerr("DAQ_Clear", error);
                                }
                status = 0;
                while ((status == 0) && (error == 0))
                                {
                                error = DAQ_Check(slot, &status); /* scan is finished when status
                                                not equal to zero */
                                chkerr("DAQ_Check", error);
                                }

                /* demultiplex the data into separate buffers per channel */
                ptr_array[0] = chanlAdata;
                ptr_array[1] = chanlBdata;

                error = SCAN_Demux(slot,NUM_CHANS,buffer,COUNT,ptr_array);
                chkerr("SCAN_Demux", error);

                /* scale the data for channel A */
                error = DAQ_Scale(slot,gain,CountperChanl,chanlAdata,volt_arrayA);
```

```c
chkerr("DAQ_Scale", error);

/* scale the data for channel B */
error1 =  DAQ_Scale(slot,gain,CountperChanl,chanlBdata,volt_arrayB);
chkerr("DAQ_Scale", error);

if (error == 0 && error1 == 0)
    {
    i = 1;
    printf("\n %3d \t %3.3f \t\t %3.3f",elap_time,volt_arrayA[i],
    volt_arrayB[i]);
    fprintf(fp,"\n %3d \t %3.3f \t\t %3.3f",elap_time,volt_arrayA[i],
    volt_arrayB[i]);
    }

if (buffer != NULL) free (buffer);
if (chanlAdata != NULL) free (chanlAdata);
if (chanlBdata != NULL) free (chanlBdata);
if (volt_arrayA != NULL) free (volt_arrayA);
if (volt_arrayA != NULL) free (volt_arrayA);

samp_no = samp_no + 1;
elap_time = samp_no * read_interval - read_interval;
k=1;

sleep(read_interval);
}

}               /* main */

}
```

```
/*
 *   chkerr.c - checks and converts the NI_DAQ_MAC error code and
 *              prints the corresponding error message
 */

#include <stdio.h>

typedef short int int16;
typedef long  int int32;
extern int16 LDSysError;        /* global system error code */

chkerr(s,err)
char *s;
int16 err;
{
    if (err) {
      if (err == -1) {
        printf("\n%s System Error %d",s,LDSysError);
        switch (err) {
        case -37:    printf("\n***bdNamErr: Bad file name for NI_DAQ_MAC");
                     printf("\n***Check the driver name string in Device Manager calls");
                     break;
        default:     printf("\n***Check Operating System Error codes.");
                     break;
                     }
         }
        else {
            printf("\n%s\n***NI_DAQ_MAC Error %d", s, err);
            printf("\n***");
            switch (err) {
                case -60:   printf("Not an NB Series board error");
                            break;
                case -61:   printf("Bad board number error");
                            break;
                case -62:   printf("Bad gain error");
                            break;
                case -63:   printf("Bad channel number error.");
                            break;
                case -64:   printf("No support error.");
                            printf("This function is not supported by the board");
                            break;
                case -65:   printf("Bad port number error");
```

54

```
                 break;
case -66:    printf("Port not configured for output error");
                 break;
case -67:    printf("Port does not support latched mode");
                 break;
case -68:    printf("Port can not be assigned to group");
                 break;
case -69:    printf("Illegal input parameter value");
                 break;
case -70:    printf("Timeout error");
                 break;
case -71:    printf("Out of Range error");
                 break;
case -72:    printf("Data Acquisition in progress error");
                 break;
case -73:    printf("Counter in use error");
                 break;
case -74:    printf("No data aquisition in progress error");
                 break;
case -75:    printf("Overflow error");
                 break;
case -76:    printf("Overrun error");
                 break;
case -77:    printf("Bad count error.");
                 printf("Count must be multiple of number of channels ");
                 break;
case -78:    printf("Bad type error");
                 break;
case -79:    printf("No Count operation error");
                 break;
case -80:    printf("Counter reserved error");
                 break;
case -81:    printf("Port assigned to group error");
                 break;
case -82:    printf("No port assigned to group error");
                 break;
case -83:    printf("Group not configured for output error");
                 break;
case -84:    printf("Group not configured for input error");
                 break;
case -85:    printf("Block digital I/O already in progress error");
                 break;
case -86:    printf("No block digital I/O in progress error");
                 break;
case -87:    printf("One group may not use external handshaking while the
             other is performing timed I/O");
```

```
                break;
case -88:  printf("DMA transfer requires port 0 in 8-bit, 0 & 1 in 16-bit, or
            all ports in 32-bit");
                break;
case -90:  printf("Bad signal direction error");
                break;
case -91:  printf("The specified RTSI trigger line is in use");
                break;
case -92:  printf("No RTSI trigger lines are available");
                break;
case -93:  printf("The specified signal is in use");
                break;
case -94:  printf("An NB-DMA-8-G card is needed for waveform
            generation");
                break;
case -95:  printf("A DMA channel is not available for use");
                break;
case -96:  printf("A setup call is required prior to this operation");
                break;
case -97:  printf("The analog output channel is in use");
                break;
case -98:  printf("A waveform load call is required prior to this operation");
                break;
case -99:  printf("The specified channel has been assigned to a group");
                break;
case -100:  printf("No waveform operation has been executed");
                break;
case -101:  printf("Only one WF_Grp_Setup call per board is allowed");
                break;
case -102:  printf("Group waveform generation is in progress");
                break;
case -103:  printf("Specified analog trigger mode is not supported.");
                break;
case -104:  printf("Specified number of analog triggers is not supported.");
                break;
case -105:  printf("Specified hystresis window is out of range from the
            specified analog trigger level.");
                break;
case -106:  printf("Shared trigger requires that data acq. and waveform gen.
            be externally triggered.");
                break;
case -107:  printf("Continuous data acquisition or waveform generation not
            possible without DMA.");
                break;
case -108:  printf("Not enough physical memory");
                break;
```

```
case -109:  printf("Specified block size in DAQ2Config invalid for rate
            selected in DAQ_Start (DMA only)");
        break;
case -110:  printf("NI_DAQ_MAC has not been configured for double-
            buffered mode");
        break;
case -111:  printf("Acquired data was overwritten in the circular double-
            buffered acquisition buffer");
        break;
case -112:  printf("The number of samples requested is not yet available");
        break;
case -113:  printf("The double buffer data acquisition completed before the
            number of samples requested was available");
        break;
case -114:  printf("Specified block size is invalid or not an integer multiple
            of number of channels");
        break;
case -115:  printf("DAQ2MemConfig was executed after DAQ2Config");
        break;
case -116:  printf("RTSI_DisConn is not needed; signal is connected to
            trigger line.");
        break;
case -117:  printf("Cannot drive a trigger signal to the I/O connector in \
                the current trigger configuration of the NB-A2100 or NB
            A2150.");
        break;
case -118:  printf("Cannot enable digital trigger from both the RTSI bus and
            the I/O connector.");
        break;
case -119:  printf("Delayed trigger mode is not supported in current trigger
            configuration of NB-A2100.");
        break;
case -120:  printf("No trigger value was found");
        break;
case -121:  printf("Analog trigger did not occur before the specified time
            expired");
        break;
case -122:  printf("Pre-triggering not allowed in combination with analog i
            nput trigger");
        break;
case -123:  printf("Specified a delay after the trigger when collecting data so
            the delay value is ignored");
        break;
case -124:  printf("Number of samples after pretrigger is not an integer
            multiple of the number of channels");
        break;
```

```
case -125:  printf("Must call MAI_Arm befor MAI_Read for external sample
            clock");
            break;
case -126:  printf("Illegal RTSI connection");
            break;
case -127:  printf("Expected data is not avalable in FIFO");
            break;
case -128:  printf("No trigger was enabled");
            break;
case -129:  printf("Operation not allowed while the board is armed -- call
            MAI_Arm to disarm first");
            break;
case -130:  printf("Not enough pre-samples were collected");
            break;
case -131:  printf("Scan interval must be the length of one sample interval
            times the number of channels being scanned + 2µsec");
            break;
case -132:  printf("Trigger position is out of range");
            break;
case -133:  printf("Total number of samples is invalid or not an even
            number");
            break;
case -134:  printf("Invalid number of pretrigger scans specified");
            break;
case -135:  printf("Invalid number of posttrigger scans specified");
            break;
case -136:  printf("Frame size exceeded maximum number of DMA
            transfers");
            break;
case -137:  printf("Invalid scan rate specified");
            break;
case -138:  printf("Scan rate is ignored when using an external sample
            clock");
            break;
case -139:  printf("Attempted to get an invalid frame or scan from the
            acquisition buffer");
            break;
case -140:  printf("DMA config error");
            break;
case -141:  printf("Gain/offset DAC value out of range during calibration");
            break;
case -142:  printf("Gain/offset calibration was unable to converge");
            break;
case -143:  printf("Unable to read value from NB-A2000  EEPROM");
            break;
case -144:  printf("Unable to write value to NB-A2000 EEPROM");
```

```
          break;
case -145:    printf("Hardware error when reading value from NB-A2000
     EEPROM");
          break;
case -146:    printf("Invalid address for NB-A2000 EEPROM read / write");
          break;
case -147:    printf("External reference value out of range during initial
     calibration");
          break;
case -148:  printf("Internal reference value out of range during initial
     calibration");
          break;
case -149:  printf("Unable to collect calibration data from board");
          break;
case -150:  printf("Hardware initialization error");
          break;
   case -151:  printf("Clock source not consistent with operation attempted");
          break;
   case -152:  printf("Sample clock signal can not be received from and driven
        on the external sample clock line simultaneously");
          break;
   case -153:  printf("Buffer size or base address is not 16 32-bit word aligned
        for use with block mode DMA");
          break;
   case -154:  printf("Board already setup for master-slave.");
          break;
   case -155:  printf("Operation failed because resource is reserved by NI-
        DAQ.");
          break;
   case -156:  printf("Operation failed because resource is reserved by the
        user.");
          break;
   case -157:  printf("Operation failed because A2150 or A2100 slot in Master
        Slave Clock Configuration.");
          break;
   case -159:  printf("Number of points selected for waveform buffer or block
        is invalid.");
          break;
   case -160:  printf("Cannot do D/A output because the D/A FIFO is
        disabled.");
          break;
   case -161:  printf("Specified buffer number is invalid.");
          break;
   case -162:  printf("Specified group number is invalid.");
          break;
```

59

```
case -163:  printf("Cannot execute this function when buffered waveform
              generation is in progress.");
              break;
case -164:  printf("Cannot execute this function when buffered waveform
              generation has completed.");
              break;
case -165:  printf("D/A FIFO Underflow error.  If NB-DMA-8 board is
              used, RTSI cable must be connected.");
              break;
case -166:  printf("DMA chaining operation malfunctioned and halted the
              DMA process.");
              break;
case -167:  printf("Underwrite error.  Waveform data was generated more t
              than desired number of times.");
              break;
case -168:  printf("Cannot execute when last block has already been
              loaded.");
              break;
case -169:  printf("Buffered waveform generation has stopped to prevent
              regeneration of data.");
              break;
case -175:  printf("Line not configured for output in case of write.");
              break;
case -180:  printf("Could not make the virtual memory buffer contiguous for
              use in a DMA data acquisition or waveform generation.");
              break;
case -181:  printf("Analog triggering and pretriggering flags must be
              disabled before starting block mode data acquisition.");
              break;
case -182:  printf("Since external signal is used for later update mode, this
              call had no effect.");
              break;
case -183:  printf("The SCXI chassis ID does not correspond to a
              configured chassis.");
              break;
case -184:  printf("The SCXI module slot specified is invalid or
              corresponds to an empty slot.");
              break;
case -185:  printf("The NI-DAQ Preferences file could not be found or has
              been corrupted.");
              break;
case -186:  printf("The SCXI configuration parameters specified indicate\n ");
              printf("an invalid SCXI configuration, or the current function\n ");
              printf("cannot be executed because of the current SCXI
              configuration.");
              break;
```

```c
        case -187:  printf("SCXI communication error; either the chassis
                     communication is\n ");
                        printf("disabled, or the driver could not successfully
                     communicate with the chassis ");
                        break;
        case -188:  printf("Either the operating mode specified in an SCXI config
                     call is invalid,\n ");
            printf("a module is in the wrong opMode to execute the current function.");
                        break;
        case -189:  printf("One of the SCXI modules specified for a function is not
                     supported for\n");
                 printf("the operation; the rest of the function was executed for the\n");
                        printf("specified modules that are supported\n");
                        break;
        case -190:  printf("The data acquisition board specified for an SCXI \n");
                        printf("operation is the wrong board type for the operation");
                        break;
        case -191:  printf("An attempt was made to drive the Track/Hold trigger line
                     on the\n");
                        printf("SCXIbus with more than one module, or a
                SCXI_Track_Hold_Control call\n");
                        printf("was made and the Track/Hold setup is not correct \n");
                        break;
        case -300:  printf("WARNING: Wrote to a port where some lines are
                     configured for input.");
                        break;
        case -500:  printf("unexpected error");
                        break;
        default:printf("Consult NI_DAQ_MAC error codes");
                        break;
        }
    printf("\n");
        }
    }
    /*else
        printf("\n%s Ok\n", s);*/

} /* chkerr */
```